number of studies that subjects having normal fasting plasma glucose at OGTT together with high 1-h PG are followed as carefully as IGT subjects in cases of higher frequency of elevated HbA1c, hypertension, family history of diabetes, or peripheral vascular involvement [15]. In addition, 1-h PG is used in diagnosis of gestational diabetes mellitus (GDM) and risk of macrosomia and other perinatal complications [16,17].

In the present study, the insulin secretion and insulin sensitivity indices of Japanese subjects undergoing OGTT in three WHO categories, normal glucose tolerance (NGT), isolated impaired fasting glucose (IFG) and isolated impaired glucose tolerance (IGT), subdivided at 1-h PG of 10.0 mmol/l were evaluated and compared.

2. Subjects and methods

2.1. Subjects

We recruited subjects undergoing OGTT because of positive urine glucose test, >5.0% HbA1c level, >5.6 mmol/l fasting plasma glucose level, and family history of diabetes at initial examination for medical check-up at Kyoto University Hospital, Ikeda Hospital, Kansai Electric Power Hospital, Kansai Health Management Center, and Kyoto Preventive Medical Center from 1993 to 2005. Subjects in the three categories of glucose tolerance, NGT ($n = 179$: fasting plasma glucose (FPG) level < 6.1 mmol/l and 2-h PG level < 7.8 mmol/l), isolated IFG ($n = 44$: FPG level of 6.1–7.0 mmol/l and 2-h PG < 7.8 mmol/l), and isolated IGT ($n = 103$: FPG level < 6.1 mmol/l and 2-h PG level of 7.8–11.1 mmol/l) according to the diagnostic criteria of World Health Organization in 1998 [18] were enrolled in the study. All subjects were men with no signs of hypertension, hepatic or renal dysfunction, endocrine or malignant disease, engaging in heavy exercise, history of gastrectomy, or history of medication known to affect glucose metabolism. The study was designed in compliance with the ethics regulations of the Helsinki Declaration. After the subjects fasted overnight for 10–16 h, standard OGTT with 75 g glucose was administered according to the National Diabetes Data Group recommendations [16].

The three WHO categories of glucose tolerance were divided into subgroups at 1-h PG of 10.0 mmol/l in this study: NGT with higher 1-h plasma glucose (NGT-HG: NGT criteria and 1-h PG ≥10.0 mmol/l), NGT with lower 1-h plasma glucose (NGT-LG: NGT criteria and 1-h PG <10.0 mmol/l), isolated IFG with higher 1-h plasma glucose (IFG-HG: IFG criteria and 1-h PG ≥10.0 mmol/l), isolated IFG with lower 1-h plasma glucose (IFG-LG: IFG criteria and 1-h PG <10.0 mmol/l), isolated IGT with higher 1-h plasma glucose (IGT-HG: IGT criteria and 1-h PG ≥10.0 mmol/l), and isolated IGT with lower 1-h plasma glucose (IGT-LG: IGT criteria and 1-h PG <10.0 mmol/l).

2.2. Laboratory examination

Blood samples were collected at 0, 30, 60, and 120 min after OGTT, and plasma glucose and serum insulin levels were measured for all subjects. Plasma glucose and serum insulin levels at 90 min were measured for 75 NGT subjects. Blood samples for measurements of HbA1c, total cholesterol, HDL cholesterol, and triglycerides were drawn after an overnight fast.

The plasma glucose level was measured by glucose oxidase method using the Hitachi Automatic Clinical Analyzer 7170 (Hitachi, Tokyo, Japan). Serum insulin was measured by two-site radioimmunoassay (Insulin Riabead II, Dainabot, Tokyo, Japan) as reported previously [19]. Serum total cholesterol and triglycerides levels were measured as reported previously [20].

2.3. Measurement

Basal insulin secretion and sensitivity were evaluated by HOMA β-cell and HOMA-IR [21,22], respectively. Early-phase insulin secretion and systemic insulin sensitivity during OGTT were evaluated by insulinogenic index [23] and ISI composite [24,25]. The calculations were as follows:

$$\text{HOMA } \beta\text{-cell} = \frac{20 \times \text{fasting serum insulin level (FI) (mU/l)}}{\text{fasting plasma glucose level (FPG) (mmol/l)} - 3.5}$$

$$\text{HOMA-IR} = \frac{\text{FI (mU/l)} \times \text{FPG (mmol/l)}}{22.5}$$

$$\text{Insulinogenic index} = \frac{\text{30-min insulin} - \text{FI (pmol/l)}}{\text{30-min plasma glucose} - \text{FPG (mmol/l)}}$$

$$\text{ISI composite} = \frac{10{,}000}{\left[\begin{array}{l}\text{FPG (mg/dl) FI (mU/ml)} \times \text{mean OGTT glucose (mg/dl)} \\ \times \text{mean OGTT serum insulin (mU/ml)}\end{array}\right]^{0.5}}$$

2.4. Statistical analysis

All analyses were performed using STATVIEW 5 system (Stat View, Berkeley, CA). Differences between two groups were assessed by unpaired t-test in terms of age, BMI, plasma glucose level, serum insulin level, HbA1c, triglyceride, total cholesterol, insulinogenic index, ISI composite, HOMA-IR, and HOMA β-cell. We used simple regression analysis and multiple regression analysis for comparison of the relationship between 1-h PG and the indices of insulin secretion and sensitivity. Probability (p) values less than 0.05 were considered statistically significant. Data are presented as mean ± S.E.

3. Results

Table 1 shows the clinical and metabolic characteristics of the six subgroups. NGT-HG had higher average age, BMI, FPG, 2-h PG and HbA1c than NGT-LG. IFG-HG had higher BMI than IFG-LG. IGT-HG had higher BMI, FPG, 2-h PG, 1-h insulin and HbA1c than IGT-LG. There were no significant differences in insulin (fasting and 2-h), triglycerides, total cholesterol and HDL-cholesterol levels between the two subgroups of NGT, isolated IFG, and isolated IGT.

The insulin secretion indices of insulinogenic index and HOMA β-cell indices in the three WHO categories are shown in

Table 1 – Clinical characteristics of the subjects in six subgroups of three WHO categories at 10.0 mmol/l

	NGT		Isolated IFG		Isolated IGT	
	NGT-LG	NGT-HG	IFG-LG	IFG-HG	IGT-LG	IGT-HG
Total N	179		44		103	
N	121	58	14	30	32	71
Age (years)	47.2 ± 1.1	53.1 ± 1.3**	54.4 ± 2.1	51.5 ± 1.9	52.0 ± 1.6	52.2 ± 1.1
BMI (kg/m2)	23.1 ± 1	24.2 ± 0.4*	22.6 ± 0.8	24.2 ± 0.6*	22.8 ± 0.5	24.0 ± 0.3*
FPG (mmol/l)	5.2 ± 0.0	5.6 ± 0.0***	6.3 ± 0.1	6.3 ± 0.0	5.2 ± 0.1	5.6 ± 0.0***
1-h PG(mmol/l)	7.7 ± 0.1	11.5 ± 0.2***	8.2 ± 0.4	12.5 ± 0.4***	7.9 ± 0.3	12.2 ± 0.2***
2-h PG(mmol/l)	5.7 ± 0.1	6.2 ± 0.1*	6.0 ± 0.4	6.5 ± 0.1	8.6 ± 0.1	9.2 ± 0.1**
Fasting insulin(pmol/l)	31 ± 1	30 ± 2	26 ± 2	33 ± 3	34 ± 4	34 ± 2
1-h insulin(pmol/l)	250 ± 18	287 ± 23	287 ± 68	238 ± 29	146 ± 16	221 ± 18*
2-h insulin(pmol/l)	191 ± 16	196 ± 16	133 ± 17	192 ± 27	211 ± 22	254 ± 20
HbA1c(%)	5.1 ± 0.1	5.4 ± 0.1***	5.6 ± 0.1	5.6 ± 0.1	5.2 ± 0.1	5.6 ± 0.1*
Triglycerides(mmol/l)	1.28 ± 0.08	1.47 ± 0.16	1.14 ± 0.17	1.31 ± 0.15	1.74 ± 0.29	1.85 ± 0.25
Total cholesterol(mmol/l)	5.33 ± 0.1	5.31 ± 0.11	5.01 ± 0.3	5.41 ± 0.14	5.3 ± 0.16	5.41 ± 0.1
HDL-cholesterol(mmol/l)	1.45 ± 0.05	1.47 ± 0.07	1.46 ± 0.11	1.51 ± 0.11	1.37 ± 0.10	1.39 ± 0.06

* $p < 0.05$, ** $p < 0.01$, *** $p < 0.001$ vs. LG. Data are mean ± S.E.

Fig. 1A and B. The insulinogenic index in the HG groups was remarkably lower than in the LG groups. The insulinogenic index values were 25.6 ± 0.3 vs. 75.9 ± 1.6 (NGT-HG vs. NGT-LG: $p < 0.01$), 23.1 ± 0.5 vs. 67.0 ± 3.5 (IFG-HG vs. IFG-LG: $p < 0.05$) and 22.6 ± 0.3 vs. 56.4 ± 1.9 (IGT-HG vs. IGT-LG: $p < 0.01$). The HOMA-β cell index of the HG group was significantly lower than that of the LG group in NGT and isolated IGT. There was no difference between IFG-HG and IFG-LG in HOMA β-cell index. We also estimated the insulin sensitivity indices using ISI composite and HOMA-IR in the three categories. The ISI composite index represents insulin sensitivity during OGTT, while HOMA-IR represents insulin resistance at fasting state. The ISI composite and the HOMA-IR values were similar in the HG group and the LG group in all three WHO categories. ISI composite values were 7.5 ± 0.6 vs. 9.2 ± 0.4 (NGT-HG vs. NGT-LG: n.s.), 6.9 ± 0.6 vs. 8.0 ± 0.8 (IFG-HG vs. IFG-LG: n.s.) and 7.0 ± 0.4 vs. 7.8 ± 0.7 (IGT-HG vs. IGT-LG: n.s.). HOMA-IR values were 1.2 ± 0.1 vs. 1.2 ± 0.1 (NGT-HG vs. NGT-LG: n.s.), 1.4 ± 0.1 vs. 1.2 ± 0.1 (IFG-HG vs. IFG-LG: n.s.) and 1.4 ± 0.1 vs. 1.4 ± 0.1 (IGT-HG vs. IGT-LG: n.s.).

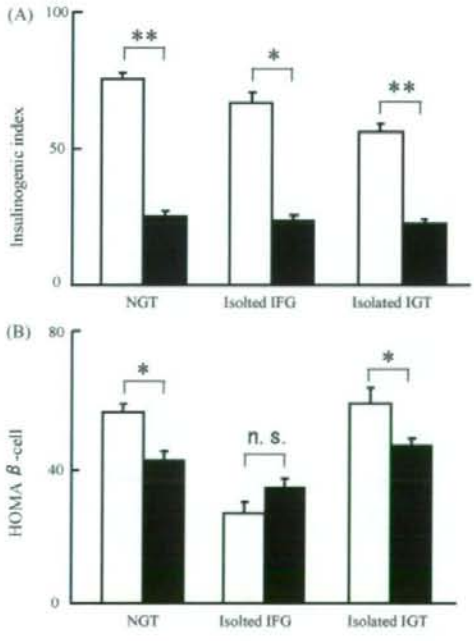

Fig. 1 – Indices of insulin secretion in six subgroups of three WHO categories: (A) insulinogenic index, (B) HOMA β-cell; light bars indicate subjects without elevated 1-h PG, dark bars indicate subjects with elevated 1-h PG. $p < 0.05$, ** $p < 0.01$, *** $p < 0.001$ vs. LG, data are mean ± S.E.

In addition, we then analyzed the relationship between 1-h PG and the indices of insulin secretion and insulin sensitivity. Scattered plots of simple regression analysis between 1-hPG and the four indices are shown in Fig. 2. 1-h PG had a significant correlation with the insulinogenic index, HOMA β-cell, and ISI composite. Multiple regression analysis revealed that HOMA β-cell, ISI composite, and insulinogenic index were the independent factors in the variation of 30.0% in 1-h PG ($p < 0.001$). The correlation coefficients of these indices with 1-h PG in simple regression analysis, and the β values and p-values of multiple regression analysis are shown in Table 2. The insulinogenic index was the strongest factor to explain the 1-h PG levels.

4. Discussion

In the present study, we found that elevated 1-h PG is strongly associated with decreased insulinogenic index, indicating reduced capacity of early-phase insulin secretion [24,25]. The insulinogenic index in NGT-HG became remarkably lower than in NGT-LG at about 20, declining to the absolute levels of IFG-HG and IGT-HG. Multiple regression analysis showed that the insulinogenic index was the strongest factor among the four indices in elevated 1-h PG. These results indicate that decreased insulinogenic index is the major factor in elevated 1-h PG during oral glucose tolerance test. Since NGT-HG showed significantly higher area under the curve of glucose

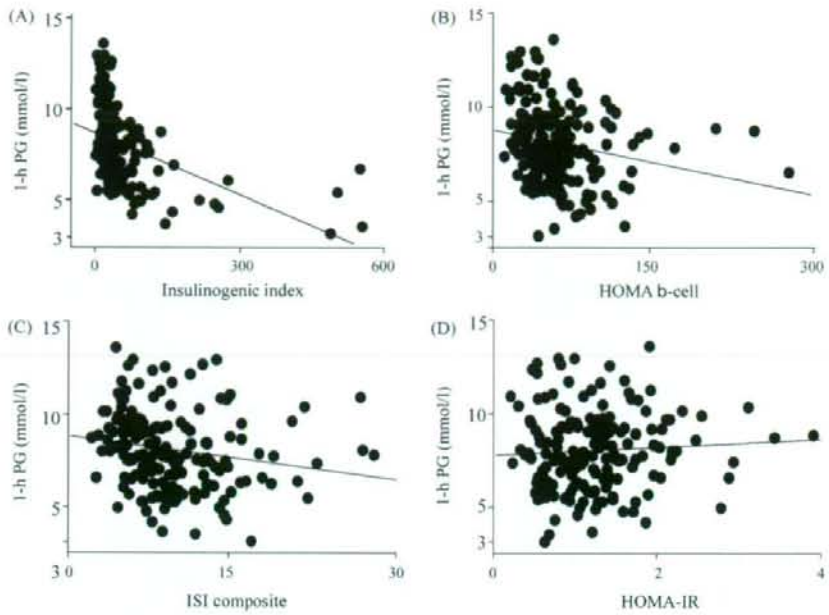

Fig. 2 – Relationship between 1-h PG and indices of insulin secretion and insulin sensitivity; (A) insulinogenic index, (B) HOMA β-cell, (C) ISI composite, (D) HOMA-IR; in insulin secretion, insulinogenic index and HOMA β-cell had significant relationships with 1-h PG ($r = -0.46$, $p < 0.001$, and $r = -0.2$, $p < 0.01$, respectively) In insulin sensitivity, there was a only mild significant relationship between 1-h PG and ISI composite ($r = -0.18$, $p < 0.05$). HOMA-IR had no significant relationship with 1-h PG ($r = 0.06$).

(G-AUC) compared to NGT-LG (19930 ± 256 vs. 15131 ± 181: $p < 0.05$), mildly impaired glucose tolerance due to reduced early-phase insulin secretion may already be present in NGT-HG. In addition, NGT-HG showed normal 2-h PG despite the elevated 1-h PG in the present study. Regarding the serum insulin level during OGTT, the 90 min insulin level in NGT-HG was significantly higher than in NGT-LG subjects (56.4 ± 7.3 vs. 40.3 ± 4.1: $p < 0.05$) in the cases we could analyze. Since late-phase insulin secretion in NGT-HG was sufficient to normalize 2-h PG, the regulatory mechanisms of elevated 1-h PG and 2-h PG are at least partly distinct.

HOMA β-cell measures insulin secretion capacity in the fasting state. HOMA β-cell values in NGT-HG and IGT-HG were significantly lower than those in NGT-LG and IGT-LG, but were similar to those in IFG-LG and IFG-HG. The values of HOMA β-cell is influenced with fasting PG per se. Isolated IFG subjects whose fasting PG levels are higher than those of NGT and isolated IGT had already low HOMA β-cell. It may explain for no significant difference between IFG-HG and IFG-LG in HOMA β-cell. Further studies are necessary to elucidate the other factors to influence HOMA β-cell in isolated IFG subjects.

Table 2 – Relationship of indices of insulin secretion and insulin sensitivity with 1-h PG

	Correlation coefficients	Standardized β	p-Value
Insulinogenic index	−0.47	0.42	<0.001
HOMA β-cell	−0.2	−0.31	<0.05
ISI composite	−0.18	−0.23	<0.05
HOMA-IR	0.06	0.13	n.s.

ISI composite and HOMA-IR are used to estimate insulin sensitivity [23]. We found both indices in LG and HG subjects to be similar in all three WHO categories. However, the insulin sensitivity of these subjects was higher than in Mexican Americans and Caucasians, as previously reported [26–28]. Since Japanese diabetes subjects are less obese than Caucasians, and insulin secretion rather than insulin sensitivity is the more important factor in the progression from NGT to diabetes in Japanese, it is likely that elevated 1-h PG in these subjects is mainly due to decreased early-phase insulin secretion rather than to impaired insulin sensitivity [19,29–31].

The ratio of NGT-HG subjects to total NGT subjects was 33% (58/121), while it was 69% (14/30) and 68% (32/71) for isolated IFG and isolated IGT subjects, respectively. The fact that the ratios increased similarly and progressively from NGT to isolated IFG and isolated IGT also suggests the use of 1-h PG as a marker to detect early stages of impaired glucose tolerance.

In conclusion, we have elucidated that impaired early-phase insulin secretion is strongly associated with an elevated 1-h PG level in Japanese subjects, suggesting that elevated 1-h PG may be a convenient marker to screen for decreased early-phase insulin secretion in early stage glucose intolerance.

Acknowledgements

This study was supported in part by Health Sciences Research Grants for Comprehensive Research on Aging and Health, and Research for Measures for Intractable Diseases from the Ministry of Health, Labour and Welfare, Leading Project of Biostimulation, and Kobe Translational Research Cluster, the Knowledge Cluster Initiative from the Ministry of Education, Culture, Sports, Science and Technology, Japan. We thank Use Techno Corporation, Ono Pharmaceutical Co. Ltd., ABBOTT JAPAN Co. Ltd, and Dainippon Sumitomo Pharmaceutical Co. Ltd for their help in the study.

Conflict of interest

There are no conflict of interest.

REFERENCES

[1] A. Mitrakou, D. Kelley, M. Mokan, T. Veneman, T. Pangburn, J. Reilly, et al., Role of reduced suppression of glucose production and diminished early insulin release in impaired glucose tolerance, N. Engl. J. Med. 2 (1992) 22–29.
[2] S.M. Haffner, M.P. Stern, H.P. Hazuda, B.D. Mitchell, J.K. Patterson, Increased insulin concentrations in nondiabetic offspring of diabetic parents, N. Engl. J. Med. 17 (1988) 1297–1301.
[3] M.F. Saad, W.C. Knowler, D. Pettitt, R.G. Nelson, M.A. Charles, P. Bennet, A two-step model for development of non-insulin-dependent diabetes, Am. J. Med. 90 (1991) 229–235.
[4] A. Taniguchi, Y. Nakai, M. Fukushima, H. Kawamura, H. Imura, I. Nagata, et al., Pathogenic factors responsible for glucose intolerance in patients with NIDDM, Diabetes 41 (1992) 1540–1546.
[5] American diabetes association, Postprandial blood glucose, Diabetes Care 24 (2001) 775–778.
[6] R.A. Defronzo, R.C. Bonadonna, E. Ferrannini, Pathogenesis of NIDDM, Diabetes Care 15 (1992) 318–368.
[7] G.T. Ko, J.K. Li, A.Y. Cheung, V.T. Yeung, C.C. Chow, L.W. Tsang, et al., Two-hour post-glucose loading plasma glucose is the main determinant for the progression from impaired glucose tolerance to diabetes in Hong Kong Chinese, Diabetes Care 22 (1999) 2096–2097.
[8] A.E. Pontiroli, P. Pizzocri, A. Caumo, G. Perseghin, L. Luzi, Evaluation of insulin release and insulin sensitivity through oral glucose tolerance test: differences between NGT, IFG, IGT, and type 2 diabetes mellitus. A cross-sectional and follow-up study, Acta Diabetol. 41 (2004) 70–76.
[9] C.W. Sisk, C.E. Burnham, J. Steward, G.W. McDonald, Comparison of the 50 and 100 gram oral glucose tolerance test, Diabetes 19 (1970) 852–862.
[10] B.R. Norman, H.B. Peter, G.S. Arthur, M. Max, Comparison of the value of the two- and one-hour glucose levels of oral GTT in the diagnosis of diabetes in Pima Indians, Diabetes 24 (1975) 538–546.
[11] T. Kuzuya, S. Nakagawa, J. Satoh, Y. Kanazawa, Y. Iwamoto, M. Kobayashi, et al., Report of the committee on the classification and diagnostic criteria of diabetes mellitus, Diabetes Res. Clin. Pract. 55 (2002) 65–85.
[12] J. Eriksson, A. Franssila-Kallunki, A. Ekstrand, C. Saloranta, E. Wide'n, C. Schalin, et al., Early metabolic defects in persons at increased risk for non-insulin-dependent diabetes mellitus, N. Engl. J. Med. 321 (1989) 337–343.
[13] J.O. Anthony, L.D. Martha, R.D. Alan, W. Molly, G. Philip, S. Jeremiah, One-hour postload plasma glucose and risks of fatal coronary heart disease and stroke among nondiabetic men and women: The Chicago Heart Association Detection Project in Industry (CHA) Study, J. Clin. Epidemiol. 50 (1997) 1369–1376.
[14] V. Olga, J.R. Karen, S. Jeremiah, Relationship of postload plasma glucose to mortality with 19-yr follow-up, Diabetes Care 15 (1992) 1328–1334.
[15] M. Michael, I.H. Maureen, M. Hillel, Evaluation of WHO and NDDG criteria for impaired glucose tolerance, Diabetes 38 (1988) 1630–1635.
[16] National Diabetes Data Group, Classification and diagnosis of diabetes mellitus and other categories of glucose intolerance, Diabetes 28 (1979) 1039–1057.
[17] American Diabetes Association, Gestational diabetes mellitus, Diabetes Care 23 (2000) S77–S79.
[18] K.G. Alberi, P.Z. Zimmeret, Definition, diagnosis and classification of diabetes mellitus and its complications. Part 1. Diagnosis and classification of diabetes mellitus provisional report of a WHO consultation, Diabet. Med. 54 (1998) 539–553.
[19] M. Fukushima, M. Usami, Y. Ikeda, A. Taniguchi, T. Matsuura, H. Suzuki, et al., Insulin secretion and insulin sensitivity at different stages of glucose tolerance: a cross-sectional study of Japanese type 2 diabetes, Metabolism 53 (2004) 831–835.
[20] A. Taniguchi, M. Fukushima, M. Sakai, K. Miwa, T. Makita, I. Nagata, et al., Remnant-like particle cholesterol, triglycerides, and insulin resistance in nonobese Japanese type 2 diabetic patients, Diabetes Care 23 (1979) 1766–1769.
[21] D.R. Matthews, J.P. Hosker, A.S. Rudenski, Homeostasis model assessment: insulin resistance and β-cell function from fasting plasma glucose and insulin concentrations in man, Diabetologia 28 (1985) 412–419.
[22] M. Fukushima, A. Taniguchi, M. Sakai, K. Doi, S. Nagasaki, H. Tanaka, et al., Homeostasis model assessment as a clinical index of insulin resistance, Diabetes Care 22 (1999) 1911–1912.
[23] M. Matsuda, R.A. Defronzo, Insulin sensitivity indices obtained from oral glucose tolerance testing: comparison with the euroglycemic insulin clamp, Diabetes Care 22 (1999) 1462–1470.
[24] H.S. Seltzer, E.W. Allen, A.L. Herron Jr., M.T. Brennan, Insulin secretion in response to glycemic stimulus: relation of delayed initial release to carbohydrate intolerance in mild diabetes mellitus, J. Clin. Invest. 46 (1967) 323–335.
[25] Y. Seino, M. Ikeda, M. Yawata, H. Imura, The insulinogenic index in secondary diabetes, Horm. Metab. Res. 7 (1975) 107–115.
[26] K.C. Chiu, L.M. Chuang, C. Yoon, Comparison of measured and estimated indices of insulin sensitivity and β cell function: impact of ethnicity on insulin sensitivity and β cell function in glucose-tolerant and normotensive subjects, J. Clin. Endocrinol. Metab. 86 (2001) 1620–1625.
[27] A. Mandavilli, D. Cyranoski, Asian's big problem, Nature Med. 10 (2004) 325–327.
[28] M. Fukushima, H. Suzuki, Y. Seino, Insulin secretion capacity in development from normal glucose tolerance to type 2 diabetes, Diabetes Res. Clin. Pract. 66 (2004) S37–S43.
[29] H. Suzuki, M. Fukushima, M. Usami, et al., Factors responsible for development from normal glucose tolerance to isolated post challenge hyperglycemia, Diabetes care 26 (2003) 1211–1215.

[30] A. Kuroe, M. Fukushima, M. Usami, M. Ikeda, A. Taniguchi, Y. Nakai, et al., Impaired beta-cell function and insulin sensitivity in Japanese subjects with normal glucose tolerance, Diabetes Res. Clin. Pract. 59 (2003) 71–77.

[31] R. Mitsui, M. Fukushima, Y. Nishi, N. Ueda, H. Suzuki, A. Taniguchi, et al., Factors responsible for deteriorating glucose tolerance in newly diagnosed type 2 diabetes in Japanese men, Metabolism 55 (2006) 53–58.

0013-7227/08/$15.00/0
Printed in U.S.A.

Endocrinology 149(2):574–579
Copyright © 2008 by The Endocrine Society
doi: 10.1210/en.2007-1292

The Murine Glucagon-Like Peptide-1 Receptor Is Essential for Control of Bone Resorption

Chizumi Yamada, Yuichiro Yamada, Katsushi Tsukiyama, Kotaro Yamada, Nobuyuki Udagawa, Naoyuki Takahashi, Kiyoshi Tanaka, Daniel J. Drucker, Yutaka Seino, and Nobuya Inagaki

Department of Diabetes and Clinical Nutrition (C.Y., Y.Y., K.T., K.Y., Y.S., N.I.), Kyoto University Graduate School of Medicine, and Core Research for Evolutional Science and Technology of Japan Science and Technology Cooperation (N.I), Kyoto 606-8507, Japan; Department of Internal Medicine (Y.Y.), Division of Endocrinology, Diabetes and Geriatric Medicine, Akita University School of Medicine, Akita 010-8543, Japan; Department of Biochemistry (N.U.) and Institute for Oral Science (N.T.), Matsumoto Dental University, Nagano 399-0781, Japan; Department of Nutrition (K.T.), Kyoto Women's University, Kyoto 605-8501, Japan; The Samuel Lunenfeld Research Institute (D.J.D.), Department of Medicine, Mount Sinai Hospital and the Banting and Best Diabetes Center, University of Toronto, Toronto, Canada M5G 2C4; Kansai Electric Power Hospital (Y.S.), Osaka 553-0003, Japan

Gastrointestinal hormones including gastric inhibitory polypeptide (GIP), glucagon-like peptide (GLP)-1, and GLP-2 are secreted immediately after meal ingestion, and GIP and GLP-2 have been shown to regulate bone turnover. We hypothesize that endogenous GLP-1 may also be important for control of skeletal homeostasis. We investigated the role of GLP-1 in the regulation of bone metabolism using GLP-1 receptor knockout (Glp-1r$^{-/-}$) mice. A combination of bone density and histomorphometry, osteoclast activation studies, biochemical analysis of calcium and PTH, and RNA analysis was used to characterize bone and mineral homeostasis in Glp-1r$^{-/-}$ and Glp-1r$^{+/+}$ littermate controls. Glp-1r$^{-/-}$ mice have cortical osteopenia and bone fragility by bone densitometry as well as increased osteoclastic numbers and bone resorption activity by bone histomorphometry. Although GLP-1 had no direct effect on osteoclasts and osteoblasts, Glp-1r$^{-/-}$ mice exhibited higher levels of urinary deoxypyridinoline, a marker of bone resorption, and reduced levels of calcitonin mRNA transcripts in the thyroid. Moreover, calcitonin treatment effectively suppressed urinary levels of deoxypyridinoline in Glp-1r$^{-/-}$, mice and the GLP-1 receptor agonist exendin-4 increased calcitonin gene expression in the thyroid of wild-type mice. These findings establish an essential role for endogenous GLP-1 receptor signaling in the control of bone resorption, likely through a calcitonin-dependent pathway. (*Endocrinology* 149: 574–579, 2008)

BONE IS CONTINUOUSLY remodeled throughout life, and osteoblastic bone formation and osteoclastic bone resorption are closely coordinated by a variety of local and systemic factors to maintain constant bone mass. Bone resorption is known to be rapidly inhibited by acute nutrient ingestion, suggesting that it might be mediated by other physiological factors, the levels of which change in response to the nutritional state such as incretins. Gastrointestinal hormones including gastric inhibitory polypeptide (GIP), glucagon-like peptide (GLP)-1, and GLP-2 are secreted immediately upon meal ingestion, although the fasting level of these peptides is low. GIP and GLP-2 are known to be involved in the regulation of bone turnover (1, 2).

The effect of GIP on bone has been extensively investigated *in vitro* and *in vivo*. The GIP receptor is expressed in osteoblasts (3), and GIP increases collagen type 1 expression and alkaline phosphatase activity in osteoblast-like cells (3) and protects osteoblasts from apoptosis (2), consistent with an anabolic effect. Recently, the presence of the GIP receptor in osteoclasts has been reported, and GIP has been shown to inhibit PTH-induced bone resorption, suggesting that a role of the postprandial rise in GIP is to stop active bone resorption such as occurs during fasting (4). The physiological importance of GIP receptor signaling on bone *in vivo* has been demonstrated using GIP receptor knockout (Gipr$^{-/-}$) mice, which exhibit a low bone mass phenotype due to both decreased bone formation and increased bone resorption (2, 5); and conversely, GIP-overexpressing transgenic mice exhibit increased bone mass (6).

GLP-2 is cosecreted with GLP-1 from L cells in the small and large intestine, and acts in the intestine to stimulate mucosal growth and nutrient absorption. Acute administration of GLP-2 decreases serum and urine markers of bone resorption in postmenopausal women (1, 7, 8), whereas bone formation appears to be unaffected by treatment with exogenous GLP-2. The effect of GLP-2 on bone has been investigated predominantly in humans, and the mechanism(s) underlying the GLP-2-mediated modulation of bone turnover remain unclear.

GLP-1 is well known as an incretin, and meal-stimulated plasma levels of GLP-1 are known to be diminished in patients with impaired glucose tolerance or type 2 diabetes (9). GLP-1 also has effects independent of insulin secretion such as inhibition of glucagon secretion and gastric emptying. In

First Published Online November 26, 2007

Abbreviations: BMC, Bone mineral content; BMD, bone mineral density; BS, bone surface; BV, bone volume; CT, computed tomography; DPD, deoxypyridinoline; ES, eroded surface; GIP, gastric inhibitory polypeptide; GLP, glucagon-like peptide; N.Mu.Oc, number of multinuclear osteoclasts; N.Oc, number of osteoclasts; TV, tissue volume; WT, wild type.

***Endocrinology* is published monthly by The Endocrine Society (http://www.endo-society.org), the foremost professional society serving the endocrine community.**

contrast to information derived from studies of GIP and GLP-2 on bone formation and resorption, the physiological role of GLP-1, if any, on bone is completely unknown. Because the GLP-1 receptor is expressed in thyroid C cells, and GLP-1 directly stimulates the secretion of calcitonin (10, 11), a potent inhibitor of osteoclastic bone resorption, GLP-1 may contribute to nutrient-mediated reduction of bone resorption.

In the present study, we have investigated the role of endogenous GLP-1 in the regulation of bone metabolism using GLP-1 receptor knockout (Glp-1r$^{-/-}$) mice. We performed morphological analyses of bones from Glp-1r$^{-/-}$ mice and wild-type (WT) littermate controls, including densitometry and histomorphometry. We also evaluated the effects of exogenous GLP-1 on thyroid C cells, and we determined the effect of calcitonin treatment in Glp-1r$^{-/-}$ mice. Taken together, our data illustrate an essential role for the GLP-1 receptor in the control of bone resorption.

Materials and Methods

Animals

Glp-1r$^{-/-}$ mice and Glp-1r$^{+/+}$ littermate WT controls were maintained on a C57BL/6 background as described previously (12). Mice were kept in cages with four to six animals per cage with free access to standard rodent diet and water. Male mice were used for all experiments. Crown to rump length was measured from tip of the nose to the end of the body. All procedures for animal care were approved by the Animal Care Committee of Kyoto University Graduate School of Medicine.

Bone densitometry and body composition analysis

For computed tomography (CT)-based analysis of bone mineral density (BMD), 10-wk-old WT and Glp-1r$^{-/-}$ mice were anesthetized with ip injections of pentobarbital sodium (Nembutal; Dainippon Pharmaceutical, Osaka, Japan). Tibiae (between proximal and distal epiphysis) and lumber spines (between L2 and L4) were scanned at 1-mm intervals using an experimental animal CT system (LaTheta LCT-100; Aloka, Tokyo, Japan). Bone mineral content (BMC) (milligrams), bone volume (cubic centimeters), and BMD (milligrams per cubic centimeter) were calculated using the LaTheta software (version 1.00). The minimum moment of inertia of cross-sectional areas (milligram-centimeters), which represents the flexural rigidity, and the polar moment of inertia of cross sectional areas (milligram-centimeters), which represents the torsional rigidity, were also calculated automatically by the LaTheta software (13). For body composition analysis, the whole bodies of 10-wk-old WT and Glp-1r$^{-/-}$ mice were scanned using the LaTheta CT system.

Bone histomorphometry

Six-week-old male mice were used for studies of bone histomorphometry as described previously (2). Briefly, mice were double labeled with sc injections of 30 mg/kg tetracycline hydrochloride (Sigma Chemical Co., St. Louis, MO) 4 d before being killed and 10 mg/kg calcein (Dojindo Co., Kumamoto, Japan) 2 d before being killed. Bones were stained with Villanueva bone stain for 7 d, dehydrated in graded concentrations of ethanol, and embedded in methyl-methacrylate (Wako Chemicals, Osaka, Japan) without decalcification. Bone histomorphometric measurements were made using a semiautomatic image analyzing system (System Supply, Ina, Japan) and a fluorescent microscope (Optiphot; Nikon, Tokyo, Japan) set at a magnification of ×400. Standard bone histomorphometrical nomenclatures, symbols, and units were used as described in the report of the American Society of Bone and Mineral Research Histomorphometry Nomenclature Committee (14).

Osteoclast and osteoblast assays

For osteoclast differentiation assay, mouse primary osteoblasts and bone marrow cells were cocultured for 7 d in α-MEM (Sigma) containing 10% fetal bovine serum in the presence or absence of 10^{-8} M 1α,25-dihydroxyvitamin D_3 with or without 10^{-5} M GLP-1 (Peptide Institute, Inc., Osaka, Japan). Cells positively stained for tartrate-resistant acid phosphatase containing more than three nuclei were counted as osteoclasts (15, 16). For pit formation assay of mature osteoclasts (16), aliquots of crude osteoclast preparations were plated on dentine slices and cultured with or without 10^{-4} M GLP-1 or 10^{-10} M calcitonin (Peptide Institute) for 48 h. The number of resorption pits was quantified under scanning electron microscopy. For osteoblast apoptosis assay, Saos-2 osteoblasts (Dainippon Pharmaceutical Co., Ltd., Osaka, Japan) were pretreated for 1 h with or without 10^{-6} M GLP-1 and then incubated for an additional 6 h in the presence or absence of 50 μM etoposide, as described previously (2).

Biochemical measurements

Total calcium concentration was measured using Spotchem SP-4420 (Arkray, Kyoto, Japan), and ionized calcium was measured using a blood gas analyzer (GEM premier 3000; Instrumentation Laboratory, Tokyo, Japan) after overnight fasting and 6 h after refeeding. Plasma insulin, leptin, and intact PTH levels were determined by ELISA kits for mouse insulin (Shibayagi, Gunma, Japan), mouse leptin (Morinaga, Yokohama, Japan) and mouse intact PTH (Immutopics Inc., San Clemente, CA). Urinary deoxypyridinoline (DPD) concentrations were measured using an ELISA kit (Quidel, San Diego, CA) before and at 4 h after single administration of 10 IU/kg eel calcitonin (Elcitonin; Asahi Kasei Pharma, Tokyo, Japan).

RNA preparation and quantitative real-time PCR

For analysis of thyroid calcitonin gene expression, mice were injected ip with the GLP-1 receptor agonist exendin-4 (Sigma) at a dose of 24 nmol/kg or the same volume of PBS 6 h before RNA isolation. Total RNA was extracted from thyroid tissue using RNeasy Mini Kit (QIAGEN, Valencia, CA). cDNAs were synthesized by SuperScript II Reverse Transcriptase system (Invitrogen, Carlsbad, CA) and subjected to quantitative real-time PCR using SYBR Green master kit and the ABI PRISM 7000 Sequence Detection System (Applied Biosystems, Foster City, CA). Primers for the calcitonin gene were calcitonin forward 5′-CTCACCAGGAAGGCATCAT-3′ and calcitonin reverse 5′- CAGCAGGCGAACTTCTTCTT-3′. The relative amount of mRNA was calculated with glyceraldehyde-3-phosphate dehydrogenase (GAPDH) mRNA as the invariant control: GAPDH forward 5′-TCGTTGATGGCAACAATCTC-3′ and GAPDH reverse 5′-AAATGGTGAAGGTCGGTGTG-3′.

Statistical analysis

Results are expressed as means ± SE. Statistical significance was assessed by ANOVA and unpaired Student's *t* test, where appropriate. A P value of <0.05 was considered to be statistically significant.

Results

Baseline characteristics of WT and Glp-1r$^{-/-}$ mice

Growth of Glp-1r$^{-/-}$ mice was similar to that of WT mice in body weight during the 50-wk observation period (supplemental Fig. 1A, published as supplemental data on The Endocrine Society's Journals Online web site at http://endo.endojournals.org). Body length and length of tibia measured at 10 and 50 wk of age were also almost identical to each other (supplemental Fig. 1, B and C). No significant difference was observed in fat mass (supplemental Fig. 1D) and lean body mass (supplemental Fig. 1E) between 10-wk-old WT and Glp-1r$^{-/-}$ mice determined by CT-based body composition analysis. Similarly, plasma leptin levels (supplemental Fig. 1F) were comparable in 10-wk-old WT and Glp-1r$^{-/-}$ mice. These data indicate that there was no difference between WT and Glp-1r$^{-/-}$ mice in body mass, body composition, or hormone levels that might affect bone mass.

Decreased cortical bone mass and diminished bone rigidity in the tibia of Glp-1r$^{-/-}$ mice

To evaluate the impact of the lack of GLP-1 receptor signaling on bone mass, we performed CT-based bone densitometry in bones of differing cortical/cancellous bone ratio. Tibia and lumber spine were used because the former has a higher cortical/cancellous bone ratio, whereas the latter has a lower cortical/cancellous bone ratio. The results are shown as total, cortical, cancellous, and trabecular bone mass in Fig. 1. There was no significant difference between WT and Glp-1r$^{-/-}$ mice in BMC (milligrams) (Fig. 1, A–D) and bone volume (cubic centimeters) (Fig. 1, E–H). Total BMD of tibia was significantly lower in Glp-1r$^{-/-}$ mice than in WT mice (WT mice, 612.97 ± 4.03 mg/cm^3; Glp-1r$^{-/-}$ mice, 570.07 ± 4.22 mg/cm^3; $P = 0.0000036$), but no significant difference was observed in total BMD of spine (Fig. 2I). Cortical BMD also was significantly decreased in Glp-1r$^{-/-}$ mice compared with WT mice in both tibia and spine (tibia: WT mice, 687.34 ± 3.57 mg/cm^3; Glp-1r$^{-/-}$ mice, 650.06 ± 10.59 mg/cm^3; $P = 0.0093$; spine: WT mice, 411.31 ± 8.77 mg/cm^3; Glp-1r$^{-/-}$ mice, 380.45 ± 6.67 mg/cm^3; $P = 0.018$) (Fig. 1J). However, cancellous and trabecular BMD were not significantly different in WT and Glp-1r$^{-/-}$ mice in both tibia and spine (Fig. 1, K and L). Reflecting the loss of cortical bone, Glp-1r$^{-/-}$ mice showed skeletal fragility by diminished bone rigidity indexes. The minimum moment of inertia of cross-sectional areas, which represents flexural rigidity, was significantly reduced in Glp-1r$^{-/-}$ mice (WT mice, 0.014 ± 0.002 mg·cm; Glp-1r$^{-/-}$ mice, 0.008 ± 0.001 mg·cm; $P = 0.022$) (Fig. 1M). Moreover, torsional rigidity as indicated by the polar moment of inertia of cross-sectional areas also was significantly diminished in Glp-1r$^{-/-}$ mice (WT mice, 0.064 ± 0.006 mg·cm; Glp-1r$^{-/-}$ mice, 0.040 ± 0.006 mg·cm; $P = 0.020$) (Fig. 1N). These results indicate that Glp-1r$^{-/-}$ mice have cortical osteopenia and bone fragility.

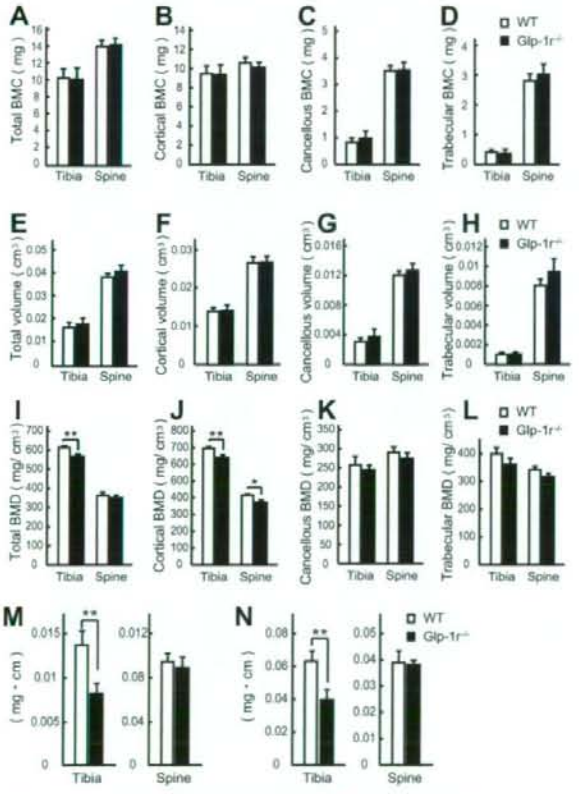

FIG. 1. CT-based bone densitometry of tibia and lumbar spine in 10-wk-old male WT (*white bars*) and Glp-1r$^{-/-}$ (*black bars*) mice. A–D, Total (A), cortical (B), cancellous (C), and trabecular (D) BMC; E–H, total (E), cortical (F), cancellous (G), and trabecular (H) BV; I–L, total (I), cortical (J), cancellous (K), and trabecular (L) BMD; M, minimum moment of inertia of cross-sectional areas, representing the flexural rigidity; N, the polar moment of inertia of cross-sectional areas, representing the torsional rigidity, calculated by LaTheta software. Values are expressed as means ± SE; n = 6 mice per group. *, $P < 0.05$; **, $P < 0.01$, WT *vs.* Glp-1r$^{-/-}$ mice.

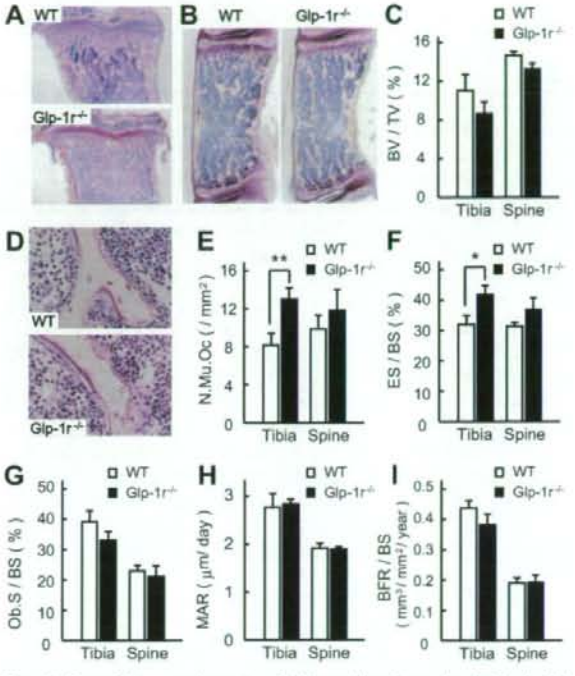

FIG. 2. Bone histomorphometry of tibia and lumbar spine in 6-wk-old male WT (*white bars*) and Glp-1r$^{-/-}$ (*black bars*) mice. A, Representative pictures of proximal tibia. Original magnification, ×20. B, Representative pictures of lumbar spine. Original magnification, ×40. C, BV/TV of tibia and lumbar spine in WT and Glp-1r$^{-/-}$ mice. D, Multinuclear osteoclasts in WT and Glp-1r$^{-/-}$ mice. Original magnification, ×400. E and F, N.Mu.Oc (E) and ES/BS (F) as cellular activity parameters regarding bone resorption. G–I, Osteoblast surface (Ob.S)/BS (G), mineral apposition rate (MAR) (H), and bone formation rate (BFR)/BS (I) as bone formation parameters. Values are expressed as means ± SE; n = 5–7 mice per group. *, $P < 0.05$; **, $P < 0.01$, WT *vs.* Glp-1r$^{-/-}$ mice.

Glp-1r$^{-/-}$ mice exhibit increased numbers of osteoclasts and bone resorption activity in the tibiae

We next performed histomorphometrical analyses of proximal tibiae (Fig. 2A) and lumbar spines (Fig. 2B) of 6-wk-old

male WT and Glp-1r$^{-/-}$ mice. Although the bone volume (BV)/tissue volume (TV) ratio (Fig. 2C) was somewhat lower in Glp-1r$^{-/-}$ mice in both tibia and spine, the difference was not statistically significant. The number of osteoclasts (N.Oc), especially multinuclear osteoclasts (N.Mu.Oc), the fully differentiated cells responsible for active bone resorption, was significantly increased in tibia of Glp-1r$^{-/-}$ mice (Fig. 2, D and E), and all of the following parameters indicating osteoclastic number were also significantly higher in the tibia of Glp-1r$^{-/-}$ mice: N.Mu.Oc per bone surface (BS) (2.06/mm^2 *vs.* 3.90/mm^2, $P = 0.022$), N.Mu.Oc per eroded surface (ES) (6.18/mm^2 *vs.* 9.32/mm^2, $P = 0.040$), N.Mu.Oc/TV (12.22/mm^2 *vs.* 20.26/mm^2, $P = 0.012$), N.Oc/BS (3.21/mm^2 *vs.* 5.98/mm^2, $P = 0.002$), and N.Oc/TV (19.28/mm^2 *vs.* 31.59/mm^2, $P = 0.009$), for WT *vs.* Glp-1r$^{-/-}$ mice, respectively. Furthermore, eroded surface (ES/BS) was significantly increased in the tibiae of Glp-1r$^{-/-}$ mice compared with WT mice (Fig. 2F). However, osteoclastic bone resorption activity was less apparent in spine of Glp-1r$^{-/-}$ mice (Fig. 2, E and F). On the other hand, no significant difference was observed in bone formation parameters, including osteoblast surface per BS (Fig. 2G), mineral apposition rate (Fig. 2H), and bone formation rate (Fig. 2I) between WT and Glp-1r$^{-/-}$ mice.

GLP-1 has no direct effect on osteoclasts and osteoblasts

Because osteoclastic number and bone resorptive activity were increased in Glp-1r$^{-/-}$ mice, we investigated whether GLP-1 has a direct effect on osteoclasts and/or osteoblasts using cell culture models. We first evaluated the effect of GLP-1 on osteoclastic differentiation by culturing bone marrow cells together with osteoblasts, because osteoclasts are formed from the precursor cells in bone marrow by stimulation from osteoblasts. As a result, GLP-1 had no inhibitory effect on 1α,25-dihydroxyvitamin D_3-induced osteoclastic generation (Fig. 3A). Pit-forming assays showed that GLP-1 had no direct effect on pit-forming activity of mature osteoclasts placed on dentine slices, whereas calcitonin completely inhibited pit formation (Fig. 3B). Unlike the GIP receptor, the GLP-1 receptor was absent in osteoblasts, and GLP-1failed to increase intracellular cAMP levels in Saos-2 cells (data not shown). Furthermore, GLP-1 had no protective effect on etoposide-induced osteoblastic apoptosis (Fig. 3C). These *in vitro* experiments demonstrate that GLP-1 has no direct effect on either osteoclasts or osteoblasts.

GLP-1 receptor signaling modulates calcitonin expression in mice

Because GLP-1 has no direct effect on bone cells, we investigated indirect pathways of GLP-1-mediated bone metabolism. Plasma levels of total calcium (data not shown) and ionized calcium (Fig. 4A) were unchanged in both fasting and fed conditions. Because hyperparathyroidism is a cause of cortical bone loss, plasma intact PTH levels were measured, but there was no difference in PTH levels between WT and Glp-1r$^{-/-}$ mice (Fig. 4B). Because the GLP-1 receptor is expressed in thyroid C cells and GLP-1 stimulates calcitonin secretion *in vitro* via a cAMP-mediated mechanism (10, 11), calcitonin could be involved in the alteration of bone metabolism observed in Glp-1r$^{-/-}$ mice. Quantitative real-time PCR analysis revealed that administration of the GLP-1 receptor agonist exendin-4 significantly increased thyroid calcitonin mRNA levels in WT mice (Fig. 4C). Conversely, the loss of GLP-1 receptor signaling in Glp-1r$^{-/-}$ mice was as-

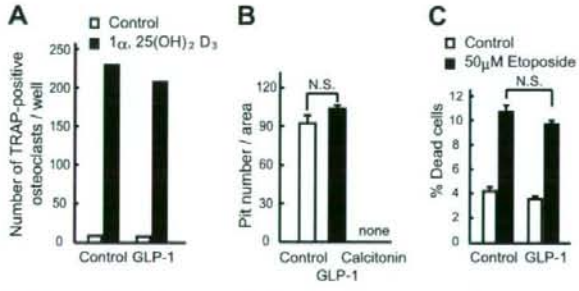

FIG. 3. Effects of GLP-1 on osteoclasts and osteoblasts *in vitro*. A, Effect of GLP-1 on osteoclastic differentiation. The numbers of tartrate-resistant acid phosphatase (TRAP)-positive osteoclasts formed from coculture of osteoblasts and bone marrow cells in the presence or absence of 10^{-8} M 1α,25-dihydroxyvitamin D_3 [1α, 25(OH)$_2$ D_3] (*white bars*)and/or 10^{-5} M GLP-1 (*black bars*) are shown. B, Effect of GLP-1 on the pit-forming activity of mature osteoclasts, using 10^{-10} M calcitonin as a positive control. C, Effect of GLP-1 on osteoblastic apoptosis. Saos-2 cells were pretreated with 10^{-4} M GLP-1 for 1 h and then incubated for an additional 6 h in the absence (*white bars*) or presence of 50 μM etoposide (*black bars*). Values are expressed as means ± SE.

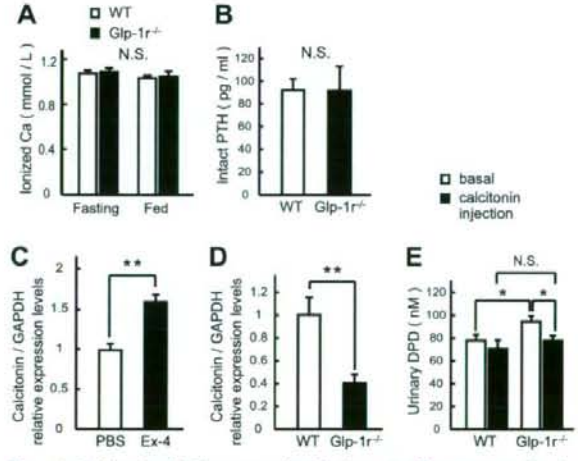

FIG. 4. Calcitonin deficiency resulted in increased bone resorption in Glp-1r$^{-/-}$ mice. A and B, Plasma levels of ionized calcium (A) and intact PTH (B) in WT and Glp-1r$^{-/-}$ mice. Values are expressed as means ± SE; n = 6–8 mice per group. C, Relative expression levels of calcitonin mRNA in thyroid from WT mice injected ip with PBS or 24 nmol/kg exendin-4 (Ex-4) 6 h before RNA isolation. Values are expressed as means ± SE; n = 5 mice per group. *, $P < 0.01$, PBS *vs.* exendin-4 treatment. D, Relative expression levels of calcitonin mRNA in thyroid from WT and Glp-1r$^{-/-}$ mice determined by quantitative real-time PCR. Values are expressed as means ± SE; n = 4 mice per group. *, $P < 0.05$; **, $P < 0.01$, WT *vs.* Glp-1r$^{-/-}$ mice. E, Urinary elimination of DPD from WT and Glp-1r$^{-/-}$ mice before and at 4 h after single administration of 10 IU/kg calcitonin. Values are expressed as means ± SE; n = 6 mice per group. *, $P < 0.05$, WT *vs.* Glp-1r$^{-/-}$ mice.

sociated with a significant reduction in levels of calcitonin mRNA transcripts, 41% of levels in control WT thyroid glands (Fig. 4D). Consistent with results of bone histomorphometry showing increased osteoclastic bone resorption, Glp-1r$^{-/-}$ mice showed significantly higher urinary DPD concentration (Fig. 4E). However, calcitonin treatment effectively decreased the urinary DPD concentration in Glp-1r$^{-/-}$ mice (Fig. 4E), demonstrating that increased bone resorption in Glp-1r$^{-/-}$ mice remains sensitive to the antiresorptive actions of calcitonin.

Discussion

Decreased BMD is a major determinant of fracture, but fracture risk in diabetic patients is often increased (17–19) and is not necessarily associated with decreased BMD. BMD in type 2 diabetes has been reported to be decreased, normal, or increased depending on various factors such as body weight or the site where BMD is measured. Body weight is one of the main determinants of BMD in both diabetic and nondiabetic subjects, suggesting that the increased BMD could be explained by the higher body weight. In the present study, there was no difference in several metabolic factors that often indirectly modulate BMD, including body weight, fat mass, or plasma levels of leptin, between WT and Glp-1r$^{-/-}$ mice.

Quantitative CT was used in the present study for the measurement of BMD because of the merits of the method with regard to distinct assessment of cortical, cancellous, and trabecular bones and to providing indexes of bone strength in live animals (13, 20). We found that total BMD of tibia, which has a higher cortical/cancellous bone ratio, was significantly lower in Glp-1r$^{-/-}$ mice and that cortical BMD at both tibia and lumbar spine was selectively reduced in Glp-1r$^{-/-}$ mice compared with WT mice. Reflecting the cortical bone loss, Glp-1r$^{-/-}$ mice showed skeletal fragility. In diabetic patients, BMD measured at sites with high cortical/cancellous bone ratio, such as distal radius or metacarpal bone, has been reported to be selectively decreased compared with sites high in cancellous bone such as lumbar spine or femoral neck (21–24). Reduced GLP-1 secretion is one of the features of type 2 diabetes (9), and it is of interest that cortical bone loss is observed in Glp-1r$^{-/-}$ mice as well as in diabetic patients. Therefore, we suppose that modulation of GLP-1 receptor signaling may theoretically contribute to regulation of bone turnover in diabetic subjects, a hypothesis that requires further testing.

We found by bone histomorphometry that genetic loss of GLP-1 receptor signaling resulted in significantly increased osteoclastic bone resorption activity, whereas the effects on bone formation parameters were less marked, similar to the changes in bone turnover induced by gastrointestinal factors. However, unlike GIP, GLP-1 had no direct effects on osteoclasts and osteoblasts as shown by the *in vitro* experiments.

Calcitonin is a known inhibitor of bone resorption and has been reported to prevent or retard bone loss in animal models of excessive bone resorption (25–28). As to the effect of calcitonin on cortical bone, calcitonin treatment has been shown to increase lumbar vertebral cortical thickness (29) and femoral cortical areas (30) in ovariectomized rats. It has been reported that the GLP-1 receptor is expressed in thyroid C cells and that GLP-1 stimulates calcitonin secretion via a cAMP-mediated mechanism in cultured C cells (10, 11); we also found that GLP-1 has a stimulatory effect on calcitonin gene expression in thyroid C cells *in vivo*, because attempts at measurement of plasma calcitonin were not successful due to sample volumes and assay sensitivity. Thus, increased osteoclastic bone resorption in Glp-1r$^{-/-}$ mice might arise indirectly from loss of GLP-1 receptor signaling on C cells, leading to calcitonin deficiency. Consistent with this hypothesis, Glp-1r$^{-/-}$ mice exhibit reduced levels of calcitonin mRNA transcripts in the thyroid. Furthermore, calcitonin treatment effectively suppressed the urinary DPD concentration in Glp-1r$^{-/-}$ mice. Taken together, these findings are consistent with an essential role for calcitonin in the regulation of bone turnover (31) and raise the possibility that modulation of GLP-1 receptor signaling may regulate bone resorption indirectly through the thyroid C cell.

In summary, our present findings demonstrate that genetic disruption of GLP-1 receptor signaling results in cortical osteopenia and bone fragility due to increased bone resorption by osteoclasts, in association with reduced thyroid calcitonin expression. Moreover, exogenous GLP-1 administration increased calcitonin expression in the thyroid glands of normal WT mice. These findings raise the possibility that clinical modulation of GLP-1 receptor signaling in human subjects, either through administration of GLP-1 receptor agonists or dipeptidyl peptidase-4 inhibitors, may indirectly regulate bone turnover in diabetic subjects. Given the recent observations of reduced bone density and increased fracture rates in diabetic subjects treated with thiazolidinediones (32, 33), more studies directed at understanding the actions of therapies that activate GLP-1 receptor signaling seem warranted.

Acknowledgments

We gratefully acknowledge Ms. Akemi Ito, Niigata Bone Science Institute, for the measurement of bone histomorphometry, and also Dr. H. Yamauchi, Japan Osteoporosis Foundation, for technical advice on calcitonin experiments.

Received September 19, 2007. Accepted November 9, 2007.

Address all correspondence and requests for reprints to: Yuichiro Yamada, M.D., Ph.D., Department of Internal Medicine, Division of Endocrinology, Diabetes, and Geriatric Medicine, Akita University School of Medicine, 1-1-1 Hondo, Akita City, Akita 010-8543, Japan. E-mail: yamada@gipc.akita-u.ac.jp.

This work was supported by Grants-in-Aid for Scientific Research from the Ministry of Education, Culture, Sports, Science, and Technology, Japan; by Health Sciences Research Grants for Comprehensive Research on Aging and Health from the Ministry of Health, Labor, and Welfare, Japan; and by an operating grant from the Juvenile Diabetes Research Foundation, Canada, to D.J.D.

Present address for K.T.: Anjo Kosei Hospital, Japan.

Disclosure Statement: The authors have nothing to disclose.

References

1. **Henriksen DB, Alexandersen P, Bjarnason NH, Vilsboll T, Hartmann B, Henriksen EE, Byrjalsen I, Krarup T, Holst JJ, Christiansen C** 2003 Role of gastrointestinal hormones in postprandial reduction of bone resorption. J Bone Miner Res 18:2180–2189
2. **Tsukiyama K, Yamada Y, Yamada C, Harada N, Kawasaki Y, Ogura M, Bessho K, Li M, Amizuka N, Sato M, Udagawa N, Takahashi N, Tanaka K, Oiso Y, Seino Y** 2006 Gastric inhibitory polypeptide as an endogenous factor

promoting new bone formation after food ingestion. Mol Endocrinol 20:1644–1651
3. **Bollag RJ, Zhong Q, Phillips P, Min L, Zhong L, Cameron R, Mulloy AL, Rasmussen H, Qin F, Ding KH, Isales CM** 2000 Osteoblast-derived cells express functional glucose-dependent insulinotropic peptide receptors. Endocrinology 141:1228–1235
4. **Zhong Q, Itokawa T, Sridhar S, Ding KH, Xie D, Kang B, Bollag WB, Bollag RJ, Hamrick M, Insogna K, Isales CM** 2007 Effects of glucose-dependent insulinotropic peptide on osteoclast function. Am J Physiol Endocrinol Metab 292:E543–E548
5. **Xie D, Cheng H, Hamrick M, Zhong Q, Ding KH, Correa D, Williams S, Mulloy A, Bollag W, Bollag RJ, Runner RR, McPherson JC, Insogna K, Isales CM** 2005 Glucose-dependent insulinotropic polypeptide receptor knockout mice have altered bone turnover. Bone 37:759–769
6. **Xie D, Zhong Q, Ding KH, Cheng H, Williams S, Correa D, Bollag WB, Bollag RJ, Insogna K, Troiano N, Coady C, Hamrick M, Isales CM** 2007 Glucose-dependent insulinotropic peptide-overexpressing transgenic mice have increased bone mass. Bone 40:1352–1360
7. **Henriksen DB, Alexandersen P, Byrjalsen I, Hartmann B, Bone HG, Christiansen C, Holst JJ** 2004 Reduction of nocturnal rise in bone resorption by subcutaneous GLP-2. Bone 34:140–147
8. **Henriksen DB, Alexandersen P, Hartmann B, Adrian CL, Byrjalsen I, Bone HG, Holst JJ, Christiansen C** 2007 Disassociation of bone resorption and formation by GLP-2: a 14-day study in healthy postmenopausal women. Bone 40:723–729
9. **Vilsboll T, Krarup T, Deacon CF, Madsbad S, Holst JJ** 2001 Reduced postprandial concentrations of intact biologically active glucagon-like peptide 1 in type 2 diabetic patients. Diabetes 50:609–613
10. **Crespel A, De Boisvilliers F, Gros L, Kervran A** 1996 Effects of glucagon and glucagon-like peptide-1-(7–36) amide on C cells from rat thyroid and medullary thyroid carcinoma CA-77 cell line. Endocrinology 137:3674–3680
11. **Lamari Y, Boissard C, Moukhtar MS, Jullienne A, Rosselin G, Garel JM** 1996 Expression of glucagon-like peptide 1 receptor in a murine C cell line: regulation of calcitonin gene by glucagon-like peptide 1. FEBS Lett 393:248–252
12. **Hansotia T, Baggio LL, Delmeire D, Hinke SA, Yamada Y, Tsukiyama K, Seino Y, Holst JJ, Schuit F, Drucker DJ** 2004 Double incretin receptor knockout (DIRKO) mice reveal an essential role for the enteroinsular axis in transducing the glucoregulatory actions of DPP-IV inhibitors. Diabetes 53:1326–1335
13. **Yamanouchi K, Yada E, Hozumi H, Ueno C, Nishihara M** 2004 Analyses of hind leg skeletons in human growth hormone transgenic rats. Exp Gerontol 39:1179–1188
14. **Parfitt AM, Drezner MK, Glorieux FH, Kanis JA, Malluche H, Meunier PJ, Ott SM, Recker RR** 1987 Bone histomorphometry: standardization of nomenclature, symbols, and units. Report of the ASBMR Histomorphometry Nomenclature Committee. J Bone Miner Res 2:595–610
15. **Udagawa N, Takahashi N, Yasuda H, Mizuno A, Itoh K, Ueno Y, Shinki T, Gillespie MT, Martin TJ, Higashio K, Suda T** 2000 Osteoprotegerin produced by osteoblasts is an important regulator in osteoclast development and function. Endocrinology 141:3478–3484
16. **Li X, Udagawa N, Itoh K, Suda K, Murase Y, Nishihara T, Suda T, Takahashi N** 2002 p38 MAPK-mediated signals are required for inducing osteoclast differentiation but not for osteoclast function. Endocrinology 143:3105–3113
17. **Schwartz AV** 2003 Diabetes mellitus: does it affect bone? Calcif Tissue Int 73:515–519
18. **Carnevale V, Romagnoli E, D'Erasmo E** 2004 Skeletal involvement in patients with diabetes mellitus. Diabetes Metab Res Rev 20:196–204
19. **Rakic V, Davis WA, Chubb SA, Islam FM, Prince RL, Davis TM** 2006 Bone mineral density and its determinants in diabetes: the Fremantle Diabetes Study. Diabetologia 49:863–871
20. **Bagi CM, Hanson N, Andresen C, Pero R, Lariviere R, Turner CH, Laib A** 2006 The use of micro-CT to evaluate cortical bone geometry and strength in nude rats: correlation with mechanical testing, pQCT and DXA. Bone 38:136–144
21. **Christensen J O, Svendsen OL** 1999 Bone mineral in pre- and postmenopausal women with insulin-dependent and non-insulin-dependent diabetes mellitus. Osteoporos Int 10:307–311
22. **Suzuki K, Sugimoto C, Takizawa M, Ishizuka S, Kikuyama M, Togawa H, Taguchi Y, Nosaka K, Seino Y, Ishida H** 2000 Correlations between bone mineral density and circulating bone metabolic markers in diabetic patients. Diabetes Res Clin Pract 48:185–191
23. **Majima T, Komatsu Y, Yamada T, Koike Y, Shigemoto M, Takagi C, Hatanaka I, Nakao K** 2005 Decreased bone mineral density at the distal radius, but not at the lumbar spine or the femoral neck, in Japanese type 2 diabetic patients. Osteoporos Int 16:907–913
24. **Suzuki K, Kurose T, Takizawa M, Maruyama M, Ushikawa K, Kikuyama M, Sugimoto C, Seino Y, Nagamatsu S, Ishida H** 2005 Osteoclastic function is accelerated in male patients with type 2 diabetes mellitus: the preventive role of osteoclastogenesis inhibitory factor/osteoprotegerin (OCIF/OPG) on the decrease of bone mineral density. Diabetes Res Clin Pract 68:117–125
25. **Wronski TJ, Yen CF, Burton KW, Mehta RC, Newman PS, Soltis EE, DeLuca PP** 1991 Skeletal effects of calcitonin in ovariectomized rats. Endocrinology 129:2246–2250
26. **Li M, Shen Y, Burton KW, DeLuca PP, Mehta RC, Baumann BD, Wronski TJ** 1996 A comparison of the skeletal effects of intermittent and continuous administration of calcitonin in ovariectomized rats. Bone 18:375–380
27. **Wallach S, Rousseau G, Martin L, Azria M** 1999 Effects of calcitonin on animal and in vitro models of skeletal metabolism. Bone 25:509–516
28. **Mochizuki K, Inoue T** 2000 Effect of salmon calcitonin on experimental osteoporosis induced by ovariectomy and low-calcium diet in the rat. J Bone Miner Metab 18:194–207
29. **Mosekilde L, Danielsen CC, Gasser J** 1994 The effect on vertebral bone mass and strength of long term treatment with antiresorptive agents (estrogen and calcitonin), human parathyroid hormone-(1–38), and combination therapy, assessed in aged ovariectomized rats. Endocrinology 134:2126–2134
30. **Giardino R, Fini M, Aldini NN, Gnudi S, Biagini G, Gandolfi MG, Mongiorgi R** 1996 Calcitonin and alendronate effects on bone quality in osteoporotic rats. J Bone Miner Res 21:S335 (Abstract)
31. **Huebner AK, Schinke T, Priemel M, Schilling S, Schilling AF, Emeson RB, Rueger JM, Amling M** 2006 Calcitonin deficiency in mice progressively results in high bone turnover. J Bone Miner Res 21:1924–1934
32. **Schwartz AV, Sellmeyer DE, Vittinghoff E, Palermo L, Lecka-Czernik B, Feingold KR, Strotmeyer ES, Resnick HE, Carbone L, Beamer BA, Park SW, Lane NE, Harris TB, Cummings SR** 2006 Thiazolidinedione use and bone loss in older diabetic adults. J Clin Endocrinol Metab 91:3349–3354
33. **Kahn SE, Haffner SM, Heise MA, Herman WH, Holman RR, Jones NP, Kravitz BG, Lachin JM, O'Neill MC, Zinman B, Viberti G** 2006 Glycemic durability of rosiglitazone, metformin, or glyburide monotherapy. N Engl J Med 355:2427–2443

***Endocrinology* is published monthly by The Endocrine Society (http://www.endo-society.org), the foremost professional society serving the endocrine community.**

Diabetologia (2008) 51:1226–1235
DOI 10.1007/s00125-008-1008-x

ARTICLE

Src activation generates reactive oxygen species and impairs metabolism–secretion coupling in diabetic Goto–Kakizaki and ouabain-treated rat pancreatic islets

R. Kominato · S. Fujimoto · E. Mukai · Y. Nakamura · K. Nabe · M. Shimodahira · Y. Nishi · S. Funakoshi · Y. Seino · N. Inagaki

Received: 18 February 2008 / Accepted: 16 March 2008 / Published online: 1 May 2008

Abstract
Aims/hypothesis Na^+/K^+-ATPase inhibition by ouabain suppresses ATP production by generating reactive oxygen species (ROS) and impairs glucose-induced insulin secretion from pancreatic islets. To clarify the signal-transducing function of Na^+/K^+-ATPase in decreasing ATP production by the generation of ROS in pancreatic islets, the involvement of Src was examined. In addition, the significance of Src activation in diabetic islets was examined.
Methods Isolated islets from Wistar rats and diabetic Goto–Kakizaki (GK) rats (a model for diabetes) were used. ROS was measured by 5-(and 6)-chloromethyl-2′,7′-dichlorofluorescein fluorescence using dispersed islet cells. After lysates were immunoprecipitated by anti-Src antibody, immunoblotting was performed.
Results Ouabain caused a rapid Tyr^{418} phosphorylation, indicating activation of Src in the presence of high glucose. The specific Src inhibitor 4-amino-5-(4-chlorophenyl)-7-(*t*-butyl)pyrazolo[3,4-*d*]pyrimidine (PP2) restored the ouabain-induced decrease in ATP content and the increase in ROS production. Both PP2 and ROS scavenger restored the impaired insulin release and impaired ATP elevation in GK islets, but had no such effect in control islets. PP2 reduced the high glucose-induced increase in ROS generation in GK islet cells but had no effect on that in control islet cells. Moreover, ouabain had no effect on ATP content and ROS production in the presence of high glucose in GK islets.
Conclusions/interpretation These results indicate that Src plays a role in the signal-transducing function of Na^+/K^+-ATPase, in which ROS generation decreases ATP production in control islets. Moreover, ROS generated by Src activation plays an important role in impaired glucose-induced insulin secretion in GK islets, in which Src is endogenously activated independently of ouabain.

Keywords ATP · GK rat · Na^+/K^+-ATPase · Pancreatic islet · ROS · Src

Abbreviations

$\Delta\Psi_m$	change in mitochondrial membrane potential
CM-DCF	5-(and 6)-chloromethyl-2′,7′-dichlorofluorescein
FCCP	carbonyl cyanide *p*-trifluoromethoxyphenylhydrazone
GK	Goto–Kakizaki
JC-1	5,5′,6,6′-tetrachloro-1,1′,3,3′-tetraethylbenzimidazolcarbocyanine iodide
KRBB	Krebs Ringer bicarbonate buffer
ROS	reactive oxygen species
PP2	4-amino-5-(4-chlorophenyl)-7-(*t*-butyl)pyrazolo[3,4-*d*]pyrimidine

Introduction

In pancreatic beta cells, intracellular glucose metabolism regulates exocytosis of insulin granules according to metabolism–secretion coupling, in which glucose-induced

R. Kominato · S. Fujimoto (✉) · E. Mukai · Y. Nakamura · K. Nabe · M. Shimodahira · Y. Nishi · S. Funakoshi · N. Inagaki
Department of Diabetes and Clinical Nutrition,
Graduate School of Medicine, Kyoto University,
54 Shogoin Kawahara-cho, Sakyo-ku,
Kyoto 606-8507, Japan
e-mail: fujimoto@metab.kuhp.kyoto-u.ac.jp

Y. Seino
Kansai Electric Power Hospital,
Osaka, Japan

mitochondrial ATP production plays an essential role [1]. Since depletion of mitochondrial DNA abolishes the glucose-induced ATP elevation, mitochondria clearly are a major source of ATP production in pancreatic beta cells [2, 3]. Glucose-induced insulin secretion from beta cells is often impaired by exposure to high concentrations of fuels including glucose, NEFAs and ketone bodies, and by administration of diabetogenic pharmacological agents, all of which involve impaired glucose-induced ATP elevation in beta cells [4–11]. Thus, reduced mitochondrial ATP production plays an important role in impaired glucose-induced insulin secretion.

Among the various agents that impair metabolism–secretion coupling in beta cells, the effects of reactive oxygen species (ROS) on glucose-induced insulin secretion have been extensively examined. Exposure to exogenous hydrogen peroxide (H_2O_2), the most abundant ROS, reduces glucose-induced insulin secretion by impairing mitochondrial metabolism in beta cells. Transient exposure to H_2O_2 suppresses the hyperpolarisation of mitochondrial membrane potential [12], the increment in insulin secretion, and the increase in ATP content induced by glucose in pancreatic beta cells [12, 13].

However, little is known of the role of endogenous ROS in impaired glucose-induced insulin secretion. Recent studies have shown that mitochondria produce endogenous ROS in beta cells under physiological and pathophysiological conditions. Exposure to high glucose increases mitochondrial ROS production [14, 15], and the superoxide content of islets from Zucker diabetic fatty rats is higher than that from Zucker lean control islets under a basal level of glucose but are relatively insensitive to high glucose [14].

Ouabain, a well-known specific inhibitor of Na^+/K^+-ATPase, decreases glucose-induced insulin release in the second phase [16]. We have found that ouabain decreases glucose-induced insulin release by reducing ATP content [17]. In addition, high glucose-induced hyperpolarisation of mitochondrial membrane potential was inhibited by ouabain. Furthermore, ouabain induced mitochondrial ROS production that was blocked by myxothiazol, an inhibitor of site III of the mitochondrial respiratory chain. Interestingly, these phenomena also occurred in Ca^{2+}- or Na^+-depleted conditions. An antioxidant, α-tocopherol, blocked the ouabain-induced ROS increase as well as the suppressive effect of ouabain on ATP production and insulin release. However, ouabain did not directly affect ATP production from the mitochondrial fraction. These results suggest that ouabain suppresses mitochondrial ATP production by generating mitochondrial ROS via signal transduction, independently of the intracellular cationic alternation, and has a suppressive effect on insulin secretion.

However, the details of Na^+/K^+-ATPase-mediated signal transduction in suppressing ATP production by the generation of mitochondrial ROS in pancreatic islets remain unknown. The binding of ouabain to Na^+/K^+-ATPase has been shown to activate Src, a non-receptor protein-tyrosine kinase, subsequently enhancing mitochondrial ROS production in cardiac myocytes [18–20]. In the present study, we investigated the involvement of Src in the signal-transducing function of Na^+/K^+-ATPase that reduces ATP production by generating mitochondrial ROS in pancreatic islets. In addition, the role of Src activation in impaired glucose-induced insulin secretion from diabetic islets was examined.

Methods

Animals Male Wistar and Goto–Kakizaki (GK) rats were obtained from Shimizu (Kyoto, Japan). The animals were fed standard laboratory chow ad libitum and allowed free access to water in an air-conditioned room with a 12 h light:12 h darkness cycle until used in the experiments. All experiments were carried out with rats aged 8–12 weeks. The animals were maintained and used in accordance with the Guidelines for Animal Experiments of Kyoto University.

Islet isolation and culture Islets of Langerhans were isolated from Wistar and GK rats by collagenase digestion as described previously [21]. Isolated islets were cultured for 12 h in RPMI 1640 medium containing 10% (vol./vol.) FCS, 100 U/ml penicillin, 100 μg/ml streptomycin and 5.5 mmol/l glucose, at 37°C in humidified air containing 5% CO_2.

Solutions The medium used for islet isolation and preincubation of intact islets was Krebs Ringer bicarbonate buffer containing (in mmol/l) 129.4 NaCl, 3.7 KCl, 2.7 $CaCl_2$, 1.3 KH_2PO_4, 1.3 $MgSO_4$, 24.8 $NaHCO_3$ (equilibrated with 5% CO_2–95% O_2, pH 7.4), and 0.2% (vol./vol.) BSA, hereafter referred to as KRBB. Ca^{2+}-free media were prepared with Ca^{2+}-free KRBB plus 1 mmol/l EGTA and 10 mmol/l HEPES (Ca^{2+}-free KRBB).

Measurement of ATP content After groups of ten islets were preincubated in KRBB with 2.8 mmol/l glucose for 30 min, they were batch-incubated for the indicated times in 0.5 ml Ca^{2+}-free KRBB with 2.8 or 16.7 mmol/l glucose with or without test materials. 4-amino-5-(4-chlorophenyl)-7-(*t*-butyl)pyrazolo[3, 4-d]pyrimidine (PP2) and α-tocopherol plus ascorbate were also included during preincubation. After immediate addition of $HClO_4$, sonication in ice-cold water for 3 min, and centrifugation, part of the supernatant fraction was mixed with HEPES and Na_2CO_3 and the ATP

content in islets was determined by luminometry as previously described [22].

Fluorescence measurement of ROS production and change in mitochondrial membrane potential ROS production and change in mitochondrial membrane potential ($\Delta\Psi_m$) in dispersed islet cells under Ca^{2+}-free conditions were measured by 5-(and 6)-chloromethyl-2′,7′-dichlorofluorescein (CM-DCF) fluorescence and 5,5′,6,6′-tetrachloro-1,1′,3,3′-tetraethylbenzimidazolcarbocyanine iodide (JC-1) fluorescence, respectively, as previously reported [17]. Fluorescence was corrected by subtracting parallel blanks in which islet cells were not loaded with probes, and is presented as a ratio with respect to the value at time zero.

Measurement of phosphorylation of Src Activation of Src in islets was determined by Western blotting after immunoprecipitation. After preincubation in KRBB containing 2.8 mmol/l glucose, islets were exposed to ouabain in Ca^{2+}-free KRBB or KRBB with 16.7 mmol/l glucose for the indicated times. After washing with ice-cold PBS, the islets were solubilised in ice-cold lysis buffer containing 10 mmol/l Tris–HCl (pH 7.2), 100 mmol/l NaCl, 1 mmol/l EDTA, 5 mmol/l sodium pyrophosphate, 0.5% sodium deoxycholate, 1% Nonidet P-40, protease inhibitor cocktail tablet (Roche, Penzberg, Germany) and phosphatase inhibitor cocktail set II (Calbiochem, Darmstadt, Germany) and sonicated. Cell lysates were centrifuged (560,000×*g* for 10 min at 4°C) to obtain crude cell extracts. Protein content of the supernatant was measured and adjusted by the Bradford method. The supernatant was mixed with 4 μg monoclonal anti-Src antibody (mouse monoclonal IgG_1, clone GD11; Upstate, Lake Placid, NY, USA) and 30 μl of washed Protein-G agarose beads, and gently rotated for 4 h at 4°C. After washing three times with ice-cold lysis buffer, immunoprecipitates were dissolved in 30 μl SDS-PAGE sample buffer (50 mmol/l Tris–HCl [pH 6.8], 2% SDS, 6% 2-mercaptoethanol, 10% glycerol, 1% bromophenol blue) and boiled for 5 min at 95°C. The samples were subjected to electrophoresis on 10% SDS-polyacrylamide gels and transferred onto nitrocellulose membrane (Schleicher and Schuell, Keene, NH, USA). After blocking with PBS containing 0.1% Tween 20 and 5% BSA (blocking buffer) overnight at 4°C, blotted membranes were incubated overnight with rabbit polyclonal anti-Src antibody (Santa Cruz Biotechnology, Santa Cruz, CA, USA) at 4°C in blocking buffer, and subsequently with anti-rabbit IgG horseradish peroxidase-conjugated secondary antibody (Amersham Biosciences, Tokyo, Japan) for 1 h prior to detection using ECL Plus (Amersham Biosciences). In the same membrane, the process was repeated for the following primary phosphospecific antibodies: rabbit polyclonal antibody to Src phosphorylated at Tyr^{418} (pY^{418}Src) or rabbit polyclonal antibody to Src phosphorylated at Tyr^{529} (pY^{529}Src; Biosource, Camarillo, CA, USA) and mouse polyclonal anti-phosphotyrosine antibody (pY; clone 4G10; Upstate). Anti-mouse IgG horseradish peroxidase-conjugated secondary antibody (Amersham Biosciences) was used to detect the mouse primary antibody.

Measurement of glucose oxidation Glucose oxidation was measured as previously described [8]. Cultured islets were preincubated in KRBB with 2.8 mmol/l glucose in the presence or absence of Src inhibitor and antioxidants at 37°C for 30 min. Twenty-five islets in a small tube were incubated at 37°C for 90 min in 150 μl Ca^{2+}-free KRBB containing 2.8 or 16.7 mmol/l glucose, test materials, and [U-^{14}C]glucose (1.85×10^4 Bq per tube) (Amersham, Buckinghamshire, UK). After 90 min incubation, the reaction was stopped, and the dpm of trapped $^{14}CO_2$ in the hydroxide of hyamine 10-X (Packard, Meriden, CT, USA) was counted.

Measurement of insulin release, insulin content and DNA content Insulin release from cultured islets was monitored using static incubation as described previously [17]. After an aliquot of incubation medium for insulin assay was taken, the islets remaining were lysed to determine insulin and DNA contents as described previously [22].

Materials RPMI 1640 medium, carbonyl cyanide p-trifluoromethoxyphenylhydrazone (FCCP), α-tocopherol and L-ascorbic acid were purchased from Sigma (St Louis, MO, USA). Luciferin-luciferase was obtained from Turner Designs (Sunnyvale, CA, USA). CM-DCFH diacetate and JC-1 were purchased from Invitrogen (Eugene, OR, USA). PP2, herbimycin A and SU6656 were purchased from Calbiochem (La Jolla, CA, USA). All other agents including ouabain were obtained from Nacalai Tesque (Kyoto, Japan).

Statistical analysis Results are expressed as means±SE. Statistical significance was evaluated by an unpaired Student's t test. $p<0.05$ was considered significant.

Results

Effect of ouabain on ATP content Exposure to 16.7 mmol/l glucose for 15 min increased ATP content compared with that in the presence of 2.8 mmol/l glucose (at 15 min, 16.7 mmol/l glucose: 17.1±0.9 vs 2.8 mmol/l glucose: 8.5±0.2 pmol/islet; $p<0.01$; Fig. 1a). For the 60 min incubation, ATP content remained high in the presence of 16.7 mmo/l glucose compared with that in the presence of 2.8 mmol/l glucose. Exposure to 1 mmol/l ouabain for

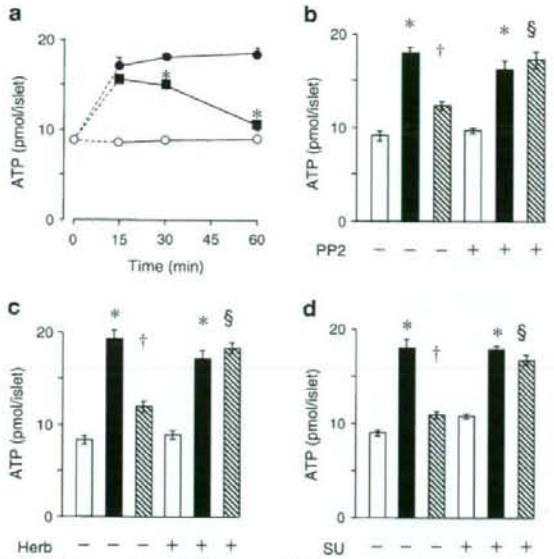

Fig. 1 Effects of Src inhibitors on ATP contents at high glucose after exposure to ouabain. **a** Time-course of ouabain-induced decrease of ATP contents. After preincubation with 2.8 mmol/l glucose, islets were incubated at 2.8 mmol/l glucose (white circles) or 16.7 mmol/l glucose with (black squares) or without (black circles) 1 mmol/l ouabain for the indicated times in Ca^{2+}-depleted condition, and ATP contents were determined. Values are means±SE (n=5). *p<0.01 vs 16.7 mmol/l glucose. **b–d** Effects of Src inhibitors on ouabain-induced decrease of ATP contents in high glucose. After preincubation with 2.8 mmol/l glucose with or without Src inhibitors, islets were incubated for 60 min at 2.8 mmol/l glucose (white bars) or 16.7 mmol/l glucose with (hatched bars) or without (black bars) ouabain in the presence or absence of Src inhibitors under Ca^{2+}-depleted condition, and ATP contents were determined. **b** Effect of 10 μmol/l PP2. **c** Effect of 1 μmol/l herbimycin A (Herb). **d** Effect of 5 μmol/l SU6656 (SU). Values are means±SE of n=8 (**b**), n=10 (**c**) and n=8 (**d**) determinations. *p<0.01 vs 2.8 mmol/l glucose; †p<0.01 vs 16.7 mmol/l glucose; §p<0.01 vs 16.7 mmol/l glucose plus ouabain without Src inhibitors

15 min did not suppress ATP content in the presence of 16.7 mmo/l glucose (at 15 min, 16.7 mmol/l glucose plus ouabain: 15.6±0.2 pmol per islet vs 16.7 mmol/l glucose; p= NS), but such exposure for 30 min decreased ATP content in the presence of 16.7 mmo/l glucose (at 30 min, 16.7 mmol/l glucose plus ouabain: 14.9±0.4 vs 16.7 mmol/l glucose: 18.0±0.4 pmol per islet; p<0.01; Fig. 1a). Furthermore, an exposure for 60 min profoundly suppressed ATP content at high glucose (at 60 min, 16.7 mmol/l glucose plus ouabain: 10.6±0.6 vs 16.7 mmol/l glucose: 18.5±0.6 pmol per islet; p<0.01; Fig. 1a).

In the presence of 10 μmol/l PP2, a Src inhibitor, 1 mmol/l ouabain failed to suppress ATP content in the presence of 16.7 mmol/l glucose (16.7 mmol/l glucose plus ouabain with PP2: 17.2±0.9 vs 16.7 mmol/l glucose with PP2: 16.2±0.9 pmol per islet; p=NS) (Fig. 1b). ATP content in ouabain-treated islets at high glucose in the presence of PP2 was larger than that in the absence of PP2 (16.7 mmol/l glucose plus ouabain with PP2 vs 16.7 mmol/l glucose plus ouabain: 12.3±0.5 pmol per islet; p<0.01). Similar results were observed in experiments using other Src inhibitors (Fig. 1c,d).

Effect of ouabain on ROS production Exposure to 1 mmol/l ouabain for 15 min did not increase CM-DCF fluorescence, which represents ROS production, in the presence of 16.7 mmo/l glucose (at 15 min, 16.7 mmol/l glucose plus ouabain: 1.23±0.11 vs 16.7 mmol/l glucose: 1.08±0.13 relative units; p=NS; Fig. 2a). However, such exposure for 30 or 60 min augmented CM-DCF fluorescence in the presence of 16.7 mmo/l glucose (at 30 min, 16.7 mmol/l glucose plus ouabain: 1.58±0.10 vs 16.7 mmol/l glucose: 1.24±0.07 relative units; p<0.05; at 60 min, 16.7 mmol/l glucose plus ouabain: 1.71±0.12 vs 16.7 mmol/l glucose: 1.29±0.04 relative units; p<0.05; Fig. 2a). In the presence of 10 μmol/l PP2, 1 mmol/l ouabain did not increase CM-DCF fluorescence in the presence of 16.7 mmol/l glucose (16.7 mmol/l glucose plus ouabain with PP2: 1.31±0.07 vs 16.7 mmol/l glucose with PP2: 1.33±0.05 relative units; p= NS) (Fig. 2b). PP2 reduced CM-DCF fluorescence of islet cells in the presence of 16.7 mmol/l glucose and 1 mmol/l ouabain (16.7 mmol/l glucose plus ouabain with PP2 vs 16.7 mmol/l glucose plus ouabain: 1.63±0.08 relative units; p<0.05; Fig. 2b).

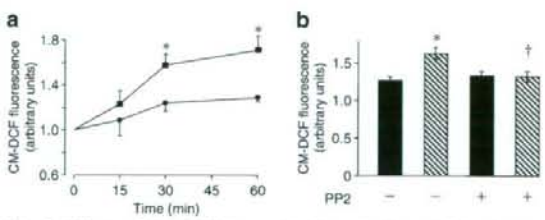

Fig. 2 Effects of Src inhibitor on ROS production at high glucose after exposure to ouabain. **a** Time-course of ouabain-induced increase of ROS production. After fluorescence measurements at time zero, the dispersed islet cells were incubated for the indicated times, with (squares) or without (circles) 1 mmol/l ouabain in the presence of 16.7 mmol/l glucose under Ca^{2+}-depleted conditions. Values are means±SE (n=4) as a ratio of values at time zero. *p<0.05 vs 16.7 mmol/l glucose. **b** Effects of Src inhibitor (PP2) on ouabain-induced increase of ROS production at high glucose. After CM-DCF fluorescence was determined at time zero, islet cells were incubated for 60 min with 16.7 mmol/l glucose with (hatched bars) or without (black bars) 1 mmol/l ouabain in the presence or absence of 10 μmol/l PP2 under Ca^{2+}-depleted conditions, and fluorescence was measured at 60 min. Values are means±SE (n=4) as a ratio of values at time zero. *p<0.05 vs 16.7 mmol/l glucose. †p<0.05 vs 16.7 mmol/l glucose plus ouabain without PP2

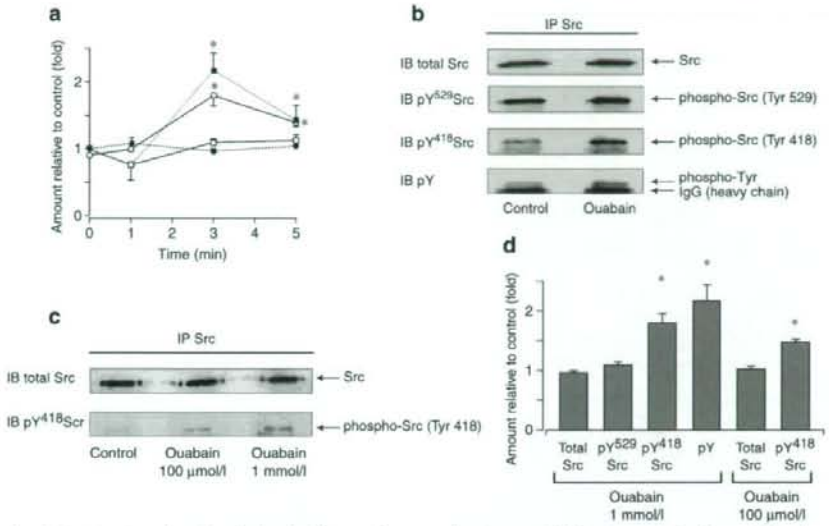

Fig. 3 Ouabain-induced Src tyrosine phosphorylation in islets under Ca^{2+}-deprived condition in the presence of 16.7 mmol/l glucose. **a** Time-course of ouabain-induced Src tyrosine phosphorylation. After preincubation with 2.8 mmol/l glucose, islets were incubated with or without 1 mmol/l ouabain in the presence of 16.7 mmol/l glucose under Ca^{2+}-depleted conditions for the indicated times. Islets were then lysed, immunoprecipitated with an anti-Src antibody, and assayed for Src tyrosine phosphorylation by Western blotting using Tyr^{418} phosphospecific Src antibody (pY^{418}Src, white circles), Tyr^{529} phosphospecific Src antibody (pY^{529}Src, white squares) or phosphotyrosine antibody (pY, black squares) by repetition of stripping and reprobing for the same blot. To ensure equal loading, total Src antibody (total Src, black circles) was also reprobed. Data are expressed relative to control (16.7 mmol/l glucose without ouabain) value (means±SE, 0 min: $n=3$, 1 min: $n=3$, 3 min: $n=8$, 5 min: $n=4$). *$p<0.01$ vs control (16.7 mmol/l glucose without ouabain). **b** Representative immunoblots (IB) for total Src antibody, Tyr^{418} or Tyr^{529} phosphospecific Src antibodies (pY^{418}Src and pY^{529}Src) and phosphotyrosine antibody (pY) at 3 min in the same membrane. In the pY immunoblot, blots of IgG heavy chain derived from antibody used during immunoprecipitation were also observed. **c** Dose-dependent effect of ouabain on the level of Src tyrosine phosphorylation in islets. Representative immunoblot (IB) for total Src antibody and pY^{418}Src antibody at 3 min in the same membrane. **d** Quantification data are expressed as means±SE of $n=6$ (100 µmol/l ouabain), $n=8$ (1 mmol/l ouabain) determinations relative to control (16.7 mmol/l glucose without ouabain) values. *$p<0.01$ vs control (16.7 mmol/l glucose without ouabain). IP, immunoprecipitated

Effect of ouabain on Src phosphorylation Src activity is regulated by the phosphorylation of Tyr^{418} and Tyr^{529}. Either a decrease in phosphorylation of Tyr^{529} or an increase in phosphorylation of Tyr^{418} stimulates Src kinase activity. Ouabain (1 mmol/l) caused a rapid activation of Src in the presence of 16.7 mmol/l glucose under Ca^{2+}-deprived conditions. The maximum increase in Tyr^{418} phospholyration was observed 3 min after ouabain exposure (Fig. 3a). Ouabain caused a significant increase in Try^{418} and total tyrosine phosphorylation, but had no effect on Try^{529} phosphorylation (at 3 min, fold increase relative to control, pY^{418}Src: 1.79±0.15, $p<0.01$ vs control; total tyrosine phosphorylation (pY): 2.17±0.26, $p<0.01$ vs control; pY^{529}Src: 1.09±0.04, p=NS vs control; total Src: 0.96±0.03, p=NS vs control) (Fig. 3b,d). A dose-dependent effect of ouabain on Tyr^{418} phosphorylation was also observed (100 µmol/l ouabain, at 3 min, fold increase relative to control, pY^{418}Src: 1.47±0.05, $p<0.01$ vs control; total Src: 1.02±0.04, p=NS vs control; Fig. 3c,d). Such effects of ouabain on Src phosphorylation were also observed in a medium containing a physiological concentration of Ca^{2+}(fold increase relative to control, pY^{418}Src: 1.59±0.10, $p<0.01$ vs control; pY^{529}Src: 1.07±0.07, p=NS vs control; total Src: 0.96±0.06, p=NS vs control) (Fig. 4).

Effect of ouabain on $\Delta\Psi_m$ To evaluate the effect of ouabain on $\Delta\Psi_m$, JC-1 fluorescence was measured in the presence of 16.7 mmol/l glucose without Ca^{2+} (Fig. 5). After addition of 16.7 mmol/l glucose to the medium, fluorescence increased gradually, indicating hyperpolarisation of mitochondrial membrane potential, whereas the basal level of fluorescence was unchanged in the presence of 2.8 mmol/l glucose. Ouabain (1 mmol/l) significantly inhibited glucose-induced hyperpolarisation of mitochondrial membrane potential 30 min after administration (at 30 min, 16.7 mmol/l glucose plus ouabain: 1.04±0.03 vs 16.7 mmol/l glucose: 1.51±0.05 relative units; $p<0.01$). However, in the presence of 1 mmol/l ouabain with 16.7 mmol/l glucose, 10 µmol/l PP2 reversed the effect of ouabain on $\Delta\Psi_m$ and increased JC-1 fluorescence 30 min

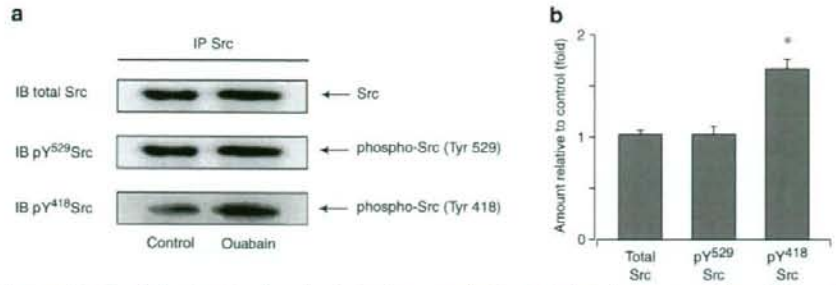

Fig. 4 Ouabain (1 mmol/l)-induced Src tyrosine phosphorylation in islets in medium containing a physiological concentration of Ca^{2+} (2.8 mmol/l) in the presence of 16.7 mmol/l glucose. **a** Representative immunoblot (IB) for total Src antibody and pY^{418}Src or pY^{529}Src antibodies at 3 min in the same membrane. **b** Quantification data from $n=5$ independent experiments. Data are expressed relative to control values (means±SE). *$p<0.01$ vs control (16.7 mmol/l glucose without ouabain). IP, immunoprecipitated

after administration (16.7 mmol/l glucose plus ouabain with PP2: 1.41±0.07 vs 16.7 mmol/l glucose plus ouabain: 1.04±0.03 relative units; $p<0.01$). JC-1 fluorescence decreased to below the basal level after the addition of 1 μmol/l FCCP.

Effect of ouabain on glucose oxidation Glucose oxidation in islets in the presence of 16.7 mmol/l glucose was increased compared with that in the presence of 2.8 mmol/l glucose (Fig. 6). Glucose oxidation with 2.8 mmol/l glucose was not affected by 1 mmol/l ouabain (ouabain plus 2.8 mmol/l glucose: 7.6±1.0 vs 2.8 mmol/l glucose: 5.6± 0.6 pmol $islet^{-1}$ 90 min^{-1}; p=NS). However, glucose oxidation with 16.7 mmol/l glucose was suppressed by the agent (16.7 mmol/l glucose plus ouabain: 30.0±4.3 vs 16.7 mmol/l glucose: 53.9±6.1 pmol $islet^{-1}$ 90 min^{-1}; $p<0.01$). In the presence of PP2 or α-tocopherol plus ascorbate, ouabain did not affect glucose oxidation at 16.7 mmol/l glucose. Glucose oxidation with 16.7 mmol/l glucose and ouabain in the presence of PP2 or α-tocopherol plus ascorbate was larger than that in the absence of PP2 and α-tocopherol plus ascorbate (16.7 mmol/l glucose plus ouabain with PP2: 50.2±4.5 vs 16.7 mmol/l glucose plus ouabain: 30.0±4.3; $p<0.01$; 16.7 mmol/l glucose plus ouabain with α-tocopherol plus ascorbate: 45.6± 3.2 pmol $islet^{-1}$ 90 min^{-1} vs 16.7 mmol/l glucose plus ouabain; $p<0.01$).

Characteristics of animals and islets Table 1 shows the characteristics of the diabetes model GK rats and control Wistar rats used in this study. GK rats had lower body weight than control Wistar rats. In the fed state, GK rats had higher plasma glucose concentration. DNA content and

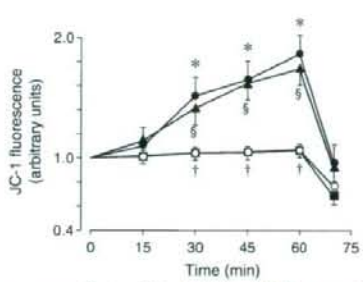

Fig. 5 Time-course effects of Src inhibitor (PP2) on ouabain-induced decrease of mitochondrial membrane potential at high glucose. After JC-1 was loaded, dispersed islet cells were preincubated for 30 min at 2.8 mmol/l glucose with or without 10 μmol/l PP2. At time zero, basal fluorescence was determined, and islet cells were incubated for the indicated time periods in Ca^{2+} -depleted conditions at 2.8 mmol/l glucose (white circles) or 16.7 mmol/l glucose with (black squares) or without (black circles) 1 mmol/l ouabain, or with 16.7 mmol/l glucose with 1 mmol/l ouabain in the presence of 10 μmol/l PP2 (black triangles). At 60 min, 1 μmol/l FCCP was added to the medium. Values are means±SE ($n=6$) as a ratio of values at time zero. *$p<0.01$, 2.8 mmol/l vs 16.7 mmol/l glucose; †$p<0.01$, 16.7 mmol/l glucose vs 16.7 mmol/l glucose + ouabain; §$p<0.01$, 16.7 mmol/l glucose + ouabain vs 16.7 mmol/l glucose + ouabain + PP2

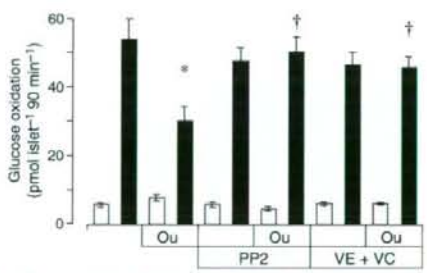

Fig. 6 Effects of Src inhibitor and ROS scavenger on ouabain-induced decrease of glucose oxidation at high glucose. After preincubation with 2.8 mmol/l glucose with or without Src inhibitor and ROS scavenger, islets were incubated for 90 min at 2.8 mmol/l glucose (white bars) or 16.7 mmol/l glucose (black bars) with or without 1 mmol/l ouabain (Ou) in the presence or absence of Src inhibitor (10 μmol/l PP2) and ROS scavenger (100 μmol/l α-tocopherol plus 200 μmol/l ascorbate, VE+VC) under Ca^{2+}-depleted conditions, and glucose oxidation was determined. Values are means ±SE of $n=11$ determinations. *$p<0.01$ vs 16.7 mmol/l glucose; †$p<0.01$ vs 16.7 mmol/l glucose plus ouabain without PP2 and α-tocopherol plus ascorbate

Table 1 Characteristics of control Wistar and diabetic GK rats used in the experiments

Characteristics	Control Wistar	GK
Bodyweight (g)	204±1 (45)	163±1** (78)
Non-fasting plasma glucose (mmol/l)	5.83±0.11 (45)	8.83±0.11** (78)
Islet DNA content (ng/islet)	13.5±0.6 (80)	13.5±0.7 (80)
Islet insulin content (ng/islet)	21.8±0.9 (80)	24.2±1.0 (80)

Data are means±SE for the number of observations shown in parentheses
**$p<0.01$ vs control Wistar rat

insulin content of islets derived from GK rats did not differ from those derived from control Wistar rats.

Effect of Src inhibition and ROS scavenger on insulin release and ATP content of GK islets In the presence of 16.7 mmol/l glucose, insulin release from GK islets was reduced compared with control Wistar rats (GK: 1.78±0.25 vs Wistar: 4.36±0.23 ng islet^{-1} 30 min^{-1}; $p<0.01$) (Fig. 7a). PP2 and α-tocopherol plus ascorbate had no effect on high glucose-induced insulin release from Wistar islets (Fig. 7a,b). However, high glucose-induced insulin release from GK islets was restored to control levels by Src inhibitor (16.7 mmol/l glucose with PP2: 5.05±0.43 vs 16.7 mmol/l glucose: 1.78±0.25 ng islet^{-1} 30 min^{-1}; $p<0.01$) and ROS scavenger (16.7 mmol/l glucose with α-tocopherol plus ascorbate: 4.22±0.60 vs 16.7 mmol/l glucose: 2.13±0.42 ng islet^{-1} 30 min^{-1}; $p<0.01$; Fig. 7a,b). The ATP content of GK islets in the presence of 2.8 mmol/l glucose was not different from that in the presence of 16.7 mmol/l glucose (2.8 mmol/l glucose: 7.0±0.4 vs 16.7 mmol/l glucose: 8.3±0.7 pmol/islet; p=NS; Fig. 7c). In GK islets, ouabain did not suppress ATP content (16.7 mmol/l glucose plus ouabain: 7.7±0.6 pmol/islet vs 16.7 mmol/l glucose; p=NS), while PP2 and α-tocopherol plus ascorbate increased ATP content in the presence of 16.7 mmol/l glucose (16.7 mmol/l glucose with PP2: 12.3±0.7 pmol/islet vs 16.7 mmol/l glucose, $p<0.01$; 16.7 mmol/l glucose with α-tocopherol plus ascorbate: 11.0±0.7 pmol/islet vs 16.7 mmol/l glucose, $p=0.01$; Fig. 7c).

Effect of Src inhibition and ROS scavenger on ROS production by GK islet cells Ouabain had no effect on ROS production in the presence of high glucose in GK islet cells (at 60 min, 16.7 mmol/l glucose plus ouabain: 2.19±0.18 vs 16.7 mmol/l glucose: 2.42±0.27 relative units; p=NS; Fig. 8a). However, PP2 and α-tocopherol plus ascorbate decreased ROS production in the presence of high glucose in GK islet cells (at 60 min, 16.7 mmol/l glucose with PP2: 1.53±0.08 relative units vs 16.7 mmol/l glucose, $p<0.05$; 16.7 mmol/l glucose with α-tocopherol plus ascorbate: 1.46±0.04 relative units vs 16.7 mmol/l glucose, $p<0.05$; Fig. 8b).

Discussion

In the present study, we show that Src plays a role in the signal-transducing function of Na^+/K^+-ATPase, by which ROS generation decreases ATP production in control islets. Moreover, ROS generated by Src activation plays an important role in impaired glucose-induced insulin secretion in GK islets, in which Src activation is ouabain independent.

In pancreatic beta cells, ROS production via non-mitochondrial and mitochondrial pathways has been proposed. ROS production from non-mitochondrial pathways including the hexosamine pathway [23], an unknown pathway from D-glyceraldehyde [24], and NADPH oxidase [25] have been reported. However, in most tissues, the major biological process leading to generation of ROS is the electron transport chain associated with the mitochondrial membrane [26, 27]. Recent studies have shown that beta cells exposed to high glucose produce mitochondrial ROS [14, 15]. Increase in ROS in the presence of high

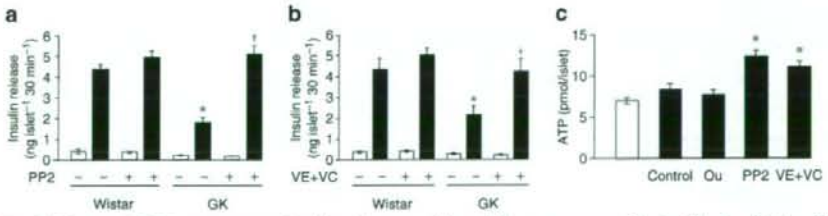

Fig. 7 Effects of Src inhibitor and ROS scavenger on insulin release and ATP contents in GK islets. After preincubation with 2.8 mmol/l glucose for 30 min, islets were incubated at 2.8 mmol/l glucose (white bars) or 16.7 mmol/l glucose (black bars) with or without test materials for 30 min (**a**, **b**) or 60 min (**c**). PP2 and α-tocopherol plus ascorbate were also included during preincubation. **a** Effects of 10 μmol/l PP2 on insulin release from control Wistar islets and GK islets. Values are means±SE (n=10). *$p<0.01$ vs Wistar, 16.7 mmol/l glucose; †$p<0.01$ vs GK, 16.7 mmol/l glucose without PP2. **b** Effects of 100 μmol/l α-tocopherol plus 200 μmol/l ascorbate (VE+VC) on ATP contents in GK islets. After incubation as indicated for 60 min in Ca^{2+}-depleted conditions, ATP contents were determined. Values are means±SE (n=10). *$p<0.01$ vs 16.7 mmol/l glucose

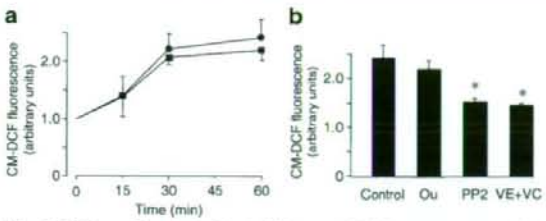

Fig. 8 Effects of ouabain, Src inhibitor and ROS scavenger on ROS production at high glucose in GK islet cells. **a** Effect of 1 mmol/l ouabain on the time-course of high glucose-induced increase of ROS production. After fluorescence measurements at time zero, the dispersed islet cells were incubated for the indicated times with (squares) or without (circles) 1 mmol/l ouabain in the presence of 16.7 mmol/l glucose under Ca^{2+}-depleted conditions. Values are means±SE (n=3) as a ratio of values at time zero. **b** Effects of 1 mmol/l ouabain (Ou), 10 μmol/l PP2 and 100 μmol/l α-tocopherol plus 200 μmol/l ascorbate (VE + VC) on ROS production in the presence of 16.7 mmol/l glucose in GK islet cells. After CM-DCF fluorescence was determined at time zero, islet cells were incubated for 60 min with 16.7 mmol/l glucose in the presence or absence of test materials under Ca^{2+}-depleted conditions, and fluorescence was measured at 60 min. Values are means±SE (n=3) as a ratio of values at time zero. *p<0.05 vs 16.7 mmol/l glucose

glucose may be attributable to $\Delta\Psi_m$-dependence of ROS formation, in which an exponential increase in ROS production is observed above 140 mV in mitochondrial membrane potential [28]. However, in the present study, we show for the first time that there is an increase in mitochondrial ROS production via intracellular signal transduction in pancreatic islets. Thus, ROS production via the signal-transducing function of Na^+/K^+-ATPase does not necessarily require hyperpolarisation of mitochondrial membrane potential, as ouabain increases ROS production while the agent simultaneously inhibits hyperpolarisation of mitochondrial membrane potential.

Src is a 60 kDa membrane-associated non-receptor tyrosine kinase that regulates various signal transduction pathways. Src production is widespread and has been demonstrated in pancreatic islets and in a beta cell line [29–32]. Its catalytic activity is controlled by tyrosine phosphorylation and protein–protein interaction. Phosphorylation of Tyr^{529} on Src holds the kinase in an inactive conformation through an intramolecular interaction with its Src homology 2 domain, whereas phosphorylation of Tyr^{418} activates Src by disrupting the intramolecular interaction and creating the substrate-binding site [33]. The binding of ouabain to the Na^+/K^+-ATPase causes rapid activation of Src in various cells including cardiac myocytes [34], smooth muscle cells [34, 35] and kidney epithelial cells [36] independently of the changes in intracellular ion concentrations. In the present study, ouabain stimulated Tyr^{418} phosphorylation but had no effect on Tyr^{529} phosphorylation, a phenomenon also observed in different types of cells [36]. Since ouabain-induced direct interaction between the Na^+/K^+-ATPase α_1 subunit and Src is observed in kidney epithelial cells [36], ouabain-induced direct interaction between Na^+/K^+-ATPase and Src may well be involved in ouabain-induced Src phosphorylation in pancreatic beta cells.

A signal-transducing function of Na^+/K^+-ATPase via Src activation has been proposed recently in different types of cells including cardiac myocytes, A7r5 cells and HeLa cells [37]. The binding of ouabain to Na^+/K^+-ATPase activates Src, resulting in transactivation of the EGF receptor and increased mitochondrial production of ROS independently of changes in intracellular ion concentrations. In the present study, PP2, a specific Src inhibitor that reduces Src kinase activity and Tyr^{418} phosphorylation in rat islets [32], was found to decrease ouabain-induced ROS production, indicating that this signal-transducing function of Na^+/K^+-ATPase plays a role in regulating mitochondrial ROS production in islets. However, the involvement of the transactivation of the EGF receptor in this pathway in islets remains unknown.

In a previous study, we found that ouabain reduces not only the increment in ATP content and the hyperpolarisation of mitochondrial membrane potential by glucose, but also the increment in O_2 consumption by glucose [17]. Since increased O_2 consumption occurs in uncoupling [38], ouabain-induced suppression of mitochondrial ATP production clearly is not mediated by uncoupling, and the suppression may derive from direct or indirect effects on the respiratory chain. Ouabain (1 mmol/l) was found to reduce glucose oxidation in the presence of 16.7 mmol/l glucose in islets in medium containing a physiological level of Ca^{2+} [39]. In the present study, 1 mmol/l ouabain also suppressed glucose oxidation in the presence of 16.7 mmol/l glucose in Ca^{2+}-depleted conditions. Since ouabain-induced suppression of glucose oxidation was restored by ROS scavenger and by Src inhibitor, increased ROS production derived from Src activation may well suppress mitochondrial metabolism in the Krebs cycle, in which CO_2 is released in the reaction mediated by dehydrogenases. This is supported by the fact that administration of 50 μmol/l H_2O_2, a concentration nearly equivalent to the 1 mmol/l ouabain-induced increase in ROS production [17], to mitochondria reduced activity of Krebs cycle enzymes including aconitase, α-ketoglutarate dehydrogenase and succinate dehydrogenase, whose activities declined 96%, 39% and 37%, respectively [40]. Considered together, these findings suggest that ouabain-induced mitochondrial ROS suppresses mitochondrial metabolism in the Krebs cycle, subsequently reducing NADH supply to the respiratory chain, hyperpolarisation of mitochondrial membrane potential, O_2 consumption and ATP production.

We then investigated the role of ROS generated by Src activation in impaired glucose-induced insulin secretion in

diabetes. One of the characteristics of type 2 diabetes is that the insulin secretory response of beta cells to glucose is selectively impaired [41]. In the GK rat, a genetic model of type 2 diabetes mellitus [42], glucose-induced insulin secretion is selectively impaired [43]. On single-channel recording, the glucose sensitivity of the beta cell K_{ATP} channel is remarkably reduced in GK rats, while the inhibitory effect of ATP on channel activity is not significantly different in control and GK rats [5]. The intracellular ATP elevation induced by high glucose is impaired in GK rats [44] as well as in patients with type 2 diabetes [45]. Thus, the impaired insulinotrophic action of glucose in beta cells of GK rats may be attributable to insufficient closure of the K_{ATP} channel because of deficient ATP production derived from impaired glucose metabolism. While there is evidence that islets in GK rats (a diabetes model) and human type 2 diabetes are oxidatively stressed [46, 47], the association between oxidative stress and impaired intracellular ATP elevation in islets is unclear. In the present study, both Src inhibitor and ROS scavenger restored the impairment in high glucose-induced insulin release and ATP elevation in GK islets but had no such effects in control islets. Moreover, Src inhibitor reduced the high glucose-induced increase in ROS generation in GK islet cells but had no effect on that in control islet cells. Ouabain had no effect on ATP content and ROS production in the presence of high glucose despite the prominent recovery effect of Src inhibitor in GK islets, suggesting that Src is endogenously activated independently of ouabain. Taken together, these results indicate that ROS generated by Src activation plays an important role in impaired glucose-induced insulin secretion derived from impaired glucose metabolism in GK islets.

Acknowledgements The authors thank T. Yamaguchi for technical assistance. This study was supported by Scientific Research Grants, a Grant for Leading Project for Biosimulation from the Ministry of Education, Culture, Sports, Science and Technology of Japan, and a grant from Core Research for Evolutional Science and Technology (CREST) of Japan Science and Technology Cooperation.

Duality of interest The authors declare that there is no duality of interest associated with this manuscript.

References

1. Maechler P, Wollheim CB (2001) Mitochondrial function in normal and diabetic β-cells. Nature 414:807–812
2. Kennedy ED, Maechler P, Wollheim CB (1998) Effects of depletion of mitochondrial DNA in metabolism secretion coupling in INS-1 cells. Diabetes 47:374–380
3. Tsuruzoe K, Araki E, Furukawa N et al (1998) Creation and characterization of a mitochondrial DNA-depleted pancreatic β-cell line: impaired insulin secretion induced by glucose, leucine, and sulfonylureas. Diabetes 47:621–631
4. Takehiro M, Fujimoto S, Shimodahira M et al (2005) Chronic exposure to β-hydroxybutyrate inhibits glucose-induced insulin release from pancreatic islets by decreasing NADH contents. Am J Physiol 288:E372–E380
5. Tsuura Y, Ishida H, Okamoto Y et al (1993) Glucose sensitivity of ATP-sensitive K^+ channels is impaired in β-cells of the GK rat. A new genetic model of NIDDM. Diabetes 42:1446–1453
6. Hughes SJ, Faehling M, Thorneley CW, Proks P, Ashcroft FM, Smith PA (1998) Electrophysiological and metabolic characterization of single β-cells and islets from diabetic GK rats. Diabetes 47:73–81
7. Anello M, Lupi R, Spampinato D et al (2005) Functional and morphological alterations of mitochondria in pancreatic beta cells from type 2 diabetic patients. Diabetologia 48:282–289
8. Nabe K, Fujimoto S, Shimodahira M et al (2006) Diphenylhydantoin suppresses glucose-induced insulin release by decreasing cytoplasmic H^+ concentration in pancreatic islets. Endocrinology 147:2717–2727
9. Radu RG, Fujimoto S, Mukai E et al (2005) Tacrolimus suppresses glucose-induced insulin release from pancreatic islets by reducing glucokinase activity. Am J Physiol 288: E365–E371
10. Patane G, Anello M, Piro S, Vigneri R, Purrello F, Rabuazzo AM (2002) Role of ATP production and uncoupling protein-2 in the insulin secretory defect induced by chronic exposure to high glucose or free fatty acids and effects of peroxisome proliferator-activated receptor-γ inhibition. Diabetes 51:2749–2756
11. Joseph JW, Koshkin V, Saleh MC et al (2004) Free fatty acid-induced β-cell defects are dependent on uncoupling protein 2 expression. J Biol Chem 279:51049–51056
12. Maechler P, Jornot L, Wollheim CB (1999) Hydrogen peroxide alters mitochondrial activation and insulin secretion in pancreatic beta cells. J Biol Chem 274:27905–27913
13. Krippeit-Drews P, Kramer C, Welker S, Lang F, Ammon HP, Drews G (1999) Interference of H_2O_2 with stimulus-secretion coupling in mouse pancreatic β-cells. J Physiol 514:471–481
14. Bindokas VP, Kuznetsov A, Sreenan S, Polonsky KS, Roe MW, Philipson LH (2003) Visualizing superoxide production in normal and diabetic rat islets of Langerhans. J Biol Chem 278:9796–9801
15. Sakai K, Matsumoto K, Nishikawa T et al (2003) Mitochondrial reactive oxygen species reduce insulin secretion by pancreatic β-cells. Biochem Biophys Res Commun 300:216–222
16. Lambert AE, Henquin JC, Malvaux P (1974) Cationic environment and dynamics of insulin secretion. IV. Effect of ouabain. Horm Metab Res 6:470–475
17. Kajikawa M, Fujimoto S, Tsuura Y et al (2002) Ouabain suppresses glucose-induced mitochondrial ATP production and insulin release by generating reactive oxygen species in pancreatic islets. Diabetes 51:2522–2529
18. Kometiani P, Li J, Gnudi L, Kahn BB, Askari A, Xie Z (1998) Multiple signal transduction pathways link Na^+/K^+-ATPase to growth-related genes in cardiac myocytes. J Biol Chem 273:15249–15256
19. Xie Z, Kometiani P, Liu J, Li J, Shapiro JI, Askari A (1999) Intracellular reactive oxygen species mediate the linkage of Na^+/K^+-ATPase to hypertrophy and its marker genes in cardiac myocytes. J Biol Chem 274:19323–19328
20. Liu J, Tian J, Haas M, Shapiro JI, Askari A, Xie Z (2000) Ouabain interaction with cardiac Na^+/K^+-ATPase initiates signal cascades independent of changes in intracellular Na^+ and Ca^{2+} concentrations. J Biol Chem 275:27838–27844
21. Fujimoto S, Ishida H, Kato S et al (1998) The novel insulinotropic mechanism of pimobendan: direct enhancement of the exocytotic process of insulin secretory granules by increased Ca^{2+} sensitivity in β-cells. Endocrinology 139:1133–1140